THE REPLICASE ASSOCIATED *CUCUMBER NECROSIS VIRUS* P33 TARGETS TO PEROXISOMES AND IS ASSOCIATED WITH THE INDUCTION OF NECROSIS IN AGRO-INFILTRATED PLANTS.

by

BHAVANA SINGH

M.Sc., GBPUA&T, Pantnagar India, 2000

B.Sc., GBPUA&T, Pantnagar India, 1998

A THESIS SUBMITTED IN PARTIAL FULFILMENT OF

THE REQUIREMENTS FOR THE DEGREE OF

MASTER OF SCIENCE

in

THE FACULTY OF GRADUATE STUDIES

(PLANT SCIENCE)

THE UNIVERSITY OF BRITISH COLUMBIA

December, 2005

Abstract

Replication of *Cucumber necrosis virus* (CNV) RNA requires two viral-encoded proteins, p33 and its read-through product p92, both of which are believed to be components of CNV replicase enzyme. In this study we have investigated the subcellular location of CNV p33 in order to gain further insight into the CNV replication process. A p33/GFP fusion protein was cloned in an *Agrobacterium tumefaciens* binary vector and used to agroinfiltrate leaves of *Nicotiana benthamiana.* Co-infiltration experiments using a YFP-labeled peroxisomal marker (pYFP-SKL) along with confocal microscopy showed that the p33/GFP fusion protein targets to the peroxisomal membrane. In addition, peroxisomes of p33/GFP inoculated cells often showed a high level of aggregation. We also report that patches of necrosis-like symptoms develop on p33/GFP infiltrated leaves suggesting that p33 contributes to the necrotic symptoms typically observed in CNV-infected plants. Similar agroinfiltration experiments were conducted with CNV p20 which is the viral suppressor of gene silencing and a protein previously suggested to modulate symptom induction. The results indicate that p20 is not capable of inducing necrotic-like symptoms on its own in agroinfiltrated plants. Phenol red assays to assess hydrogen peroxide production in leaf samples failed to show a clear correlation between necrosis and levels of peroxide accumulation in control and p33/GFP infiltrated plants. However, the DAB staining method indicated that peroxide accumulation occurred in p33/GFP infiltrated and CNV infected plants but not control plants. The association of CNV p33 with peroxisomes and its ability to induce necrosis-like symptoms in infiltrated plants suggests that p33 may contribute to the necrotic-like reaction via disruption of peroxisomal function. However, the involvement of peroxide accumulation in necrosis will require further experimentation.

Table of Contents

Abstract.....ii

Table of Contents.....iii

List of Tables.....v

List of Figures.....vi

List of Abbreviations.....vii

Acknowledgement.....x

CHAPTER 1-Introduction.....1

1.1 Purpose of study.....1

1.2 Significance of study.....2

1.3 Project objectives.....3

CHAPTER 2-Literature Review.....4

2.1 Cucumber necrosis virus.....4

2.2 Intracellular replication sites of plus-strand RNA viruses.....6

2.2.1 Association of replicase complex with membrane containing structures.....6

2.2.2. Localization of replication proteins in the virus infected cells.....10

2.3 Replication of tombusviruses.....12

2.3.1 The subcellular site of replication.....12

2.3.2. Tombusvirus replication complexes.....13

2.4 Symptom induction by plant viruses.....14

CHAPTER 3- Materials And Methods.....16

3.1 PCR amplification of p33, p20, GFP and YFP-SKL sequences.....16

3.2 Plasmid construction.....17

3.3 *Agrobacterium*-mediated transient expression.....20

3.4 Isolation and biochemical treatment of membranes.....21

3.5 Western-blot analysis.....22

3.6 Detection of hydrogen peroxide.....22

3.7 Confocal Microscopy.....23

3.8 Plant inoculations with viral RNA transcripts.....24

CHAPTER 4-Results.....25

4.1 GFP-tagged CNV p33 associates with peroxisomes in agroinfiltrated leaves of *N. benthamiana*.....25

4.2 The p33/GFP fusion protein associates with membranes in infiltrated plants.....30

4.3 The p33/GFP fusion protein is tightly associated with membranes 31

4.4 *N. benthamiana* leaves agroinfiltrated with p33/GFP develop necrotic-like patches.....31

4.5 Phenol red assays to assess hydrogen peroxide production in leaf samples do not show a clear correlation between necrosis and levels of peroxide accumulation in control and p33/GFP infiltrated plants 32

4.6 *N. benthamiana* leaves agroinfiltrated with p20/GFP do not develop necrotic patches.....37

CHAPTER 5-Discussion.....39

5.1 CNV p33/GFP targets to peroxisomes in agroinfiltrated plants.....39

5.2 CNV p33 is an integral membrane protein.....40

5.3 CNV p33 does not contain a clearly identifiable peroxisome targeting signal.....41

5.4 CNV p33 may be involved in the induction of necrosis in infected plants.....44

5.5 Does CNV p33 expression in *N. benthamiana* result in hydrogen peroxide production?.....46

Bibliography.....51

List of Tables

Table 2.1. Organellar origin of MVBs induced by several tombusviruses.....11

Table 3.1. Oligonucleotides used in this study 19

List of Figures

Fig.2.1. Linear representation of the CNV RNA genome structure..... 5

Fig. 2.2.a. Diagrammatic representation of spherules and the viral RNA replication complex.....8

Fig. 2.2.b. A general scheme for replication of a positive-strand RNA virus.....9

Fig. 3.1. Schematic representation of the pBINPLUS fusion protein expression constructs.18

Fig. 4.1. GFP-tagged CNV p33 localizes to the peroxisomal membrane in agroinfiltrated leaves of *N. benthamiana.* 26

Fig. 4.2. The p33/GFP fusion protein associates with membranes in infiltrated *N. benthamiana* plants. 28

Fig. 4.3. The p33/GFP fusion protein is tightly associated with membranes..... 29

Fig. 4.4. *N. benthamiana* leaves agroinfiltrated with p33/GFP develop necrotic-like patches. 34

Fig. 4.5. p33/GFP infiltrated *N. benthamiana* leaves show a modest increase in the levels of hydrogen peroxide. 35

Fig. 4.6. p33/GFP infiltrated leaves accumulate peroxide as determined by DAB staining..36

Fig. 5.1. CNV p33 has two predicted transmembrane domains.....42

List of Abbreviations

aa	Amino acid
ATP	Adenosine triphosphate
BMV	*Brome mosaic virus*
CIRV	*Carnation Italian ring spot virus*
CNV	*Cucumber necrosis virus*
C-terminal	Carboxy terminal
CymRSV	*Cymbidium ringspot virus*
DAB	3,3'-diaminobenzidine
DI-RNA	Defective interfering RNAs.
dpi	Days post infiltration
ds	Double-stranded
EDTA	Ethylenediaminetetraacetic acid
EGFP	Enhanced green fluorescent protein
EM	Electron microscopy
ER	Endoplasmic reticulum
EYFP	Enhanced yellow fluorescent protein
g	Genomic, *gravity* , gram
GFP	Green fluorescent protein
HCV	*Hepatitis C virus*
HEPES	2-(4-(2-Hydroxyethyl)-1-piperazinyl) ethanesulfonic acid
HF	Host factor
HIV	*Human immuno deficiency syndrome virus*
HR	Hypersensitive response

HRPO	Horseradish peroxidase
kb	Kilobase
kDa	Kilodalton
LB	Luria broth
MES	2-(N-morpholino) ethanesulphonic acid
MHV	*Mouse hepatitis virus*
mPTS	Membrane peroxisome targeting signal
MVBs	Multivesicular bodies
Nos	Nopaline synthase
N-terminal	Amino terminal
OD	Optical density
ORF	Open reading frame
PAGE	Polyacrylamide gel electrophoresis
PCD	Programmed cell death
PEB	Protein extraction buffer
PMSF	Phenylmethylsulfonyl fluoride
PRS	Phenol red solution
PTS	Peroxisome targeting signal
RCNMV	*Red clover necrotic mosaic virus*
RdRp	RNA dependent RNA polymerase
sg	Subgenomic
TBSV	*Tomato bushy stunt virus*
TEV	*Tobacco etch virus*
TMDs	Trans-membrane domains
Tris–HCl	Tris – hydrochloric acid

TYMV	*Turnip yellow mosaic virus*
U	Units
wt.	Wild type
YFP	Yellow fluorescent protein

Acknowledgement

I offer my heartfelt gratitude to Dr D' Ann Rochon, research scientist at Pacific Agriculture Research Center (PARC) Summerland, Canada for her consistent guidance, enlightening inspiration and constructive criticism throughout the course of investigation. I am very grateful to my committee members, Drs. Brian Ellis, Mary Berbee and Janet K. Chantler for their encouragement and motivation. My sincere appreciation is due to Dr. Michael Weis for introducing me to the science and art of confocal microscopy.

I wish to recognize co-operation shown by Jane Theilmann, Steve Orban, Ron Reade and Liz Hui during the course of study. I am thankful to Yu Xiang for providing valuable constructs that were used as starting material for this study. I gratefully acknowledge the Department of Biotechnology, PARC, Summerland for providing research facilities and an excellent work environment.

Many thanks to Yuvonne Kolstee for her personal support and teaching several aspects of life during my stay in Canada. I am grateful to Nitin for his help, inspiration and motivation during the course of study.

I feel a deep sense of gratitude for my late mother who formed part of my vision and the happy memory of her continue to provide encouragement and inspiration to this day. I am indepted to my father for his subtle guidance and motivation. I am thankful to Pratibha and Manjul for motivation and to my younger sisters Kamana and Arti for support and love. Finally, I owe my gratitude to Yash for helping me type this manuscript.

1. Introduction

Unraveling the molecular mechanisms underlying the complex process of RNA virus replication is important for the development of antiviral strategies. Insights into the overall multiplication cycle of RNA viruses have arisen from recent advances in the identification and function of viral RNA replication factors, the nature of the viral RNA replication complex as a membrane-bounded compartment, and the identification of host proteins that contribute to viral RNA replication. However, several stages of the virus replication cycle remain incompletely characterized and therefore cannot be adequately exploited in antiviral strategies. These include, among others, details on membrane targeting and the association of replication complexes with specific host membranes which is common to all positive-strand RNA viruses. In addition, few studies have addressed the possible specific effects of cellular organelle dysfunction that might be associated with the site of viral RNA replication and how this may relate to symptom induction in plant cells.

1.1. Purpose of the study.

Tombusviruses are small plus-strand RNA viruses that have been shown to induce multivesicular bodies (MVBs) in plant cells, with different tombusvirus species being shown to form MVBs in different organelles such as chloroplasts, mitochondria or peroxisomes. An overall goal of the studies conducted in this laboratory has been to understand the multiplication cycle of *Cucumber necrosis virus* (CNV), particularly with regards to the viral uncoating process and subsequent targeting of the virion RNA to the

site of translation and replication. Towards this, work in Dr. Rochon's laboratory has recently shown that the CNV coat protein (CP) targets to chloroplasts in *N. benthamiana* cells and that this targeting may reflect the site of CNV particle disassembly. In consideration of this finding, along with the finding that some tombusviruses may replicate in association with chloroplasts, it was of interest to determine where the intracellular site of CNV replication is in *N. benthamiana.*

1.2. Significance of the study.

Positive-strand RNA viruses are responsible for numerous clinically and economically important diseases in humans, animals, and plants. One feature shared by positive-strand RNA viruses is assembly of replication complexes on intracellular membranes with associated membrane proliferation and vesicle formation (Schwartz *et al.*, 2004). Understanding the mechanisms that target replication proteins and templates to specific intracellular membranes could lead to the development of potential antiviral strategies. The need to continuously develop new antiviral drugs to combat viruses such as *Human immunodeficiency virus* and *Hepatitis C virus* is partly due to the high error (mutation) frequency of the viral replicase which enables rapid adaptation of the virus to new selection pressures, such as antiviral drugs. Thus strategies that interfere with the viral RNA replication process could be used to minimize the opportunity for replicase-induced mutations and consequent antiviral drug resistance. The data presented in this thesis deepens our understanding of the site of viral RNA replication in a cell. This knowledge will contribute to the understanding of fundamental aspects of positive-strand

RNA virus replication, and thereby assist in strategies aimed to interfere with these processes.

1.3. Project objectives

The main objective of this study was to identify the intracellular targeting site of the CNV replicase associated protein p33 in *N. benthamiana* in order to address the possible site of viral RNA replication and to contribute to the laboratory's overall goal of achieving an in-depth understanding of the CNV multiplication process in cells. During the course of these studies it was found that CNV p33 targeted to peroxisomes, and that targeting was associated with the induction of necrosis-like symptoms in leaves, a reaction typical of CNV infection in this plant. Due to the potential significance of this observation with regards to CNV symptom development in infected plants, it became of interest to assess if targeting of p33 to peroxisomes might be responsible for the induction of necrosis via disruption of the peroxisome function in peroxide metabolism. Therefore an additional objective of this thesis was to assess whether peroxisome dysfunction occurs in p33/GFP infiltrated leaves.

2. Literature Review

2.1. *Cucumber necrosis virus*

Cucumber necrosis virus (CNV) a member of the genus *Tombusvirus*, family *Tombusviridae*, is a small, 30 nm icosahedral virus. The complete CNV genome has been cloned and sequenced (Rochon *et al.,* 1989). The genome is composed of a single positive-strand RNA molecule of 4701 nucleotides (Gene bank Accession number NC_001469) and contains five functional open reading frames (ORFs) encoding proteins designated p33, p92, p41, p21, and p20 (Fig. 2.1). Read-through of the amber stop codon that terminates the ORF1 product (p33) results in the synthesis of the putative RNA polymerase (p92) from ORF2 (Rochon *et al.,* 1991). The p41 product of ORF3 is the viral coat protein. It is translated from a 2.1 kb subgenomic RNA which is generated from the 3' terminus of the CNV genome during replication. The p21 product of ORF4 and p20 product of ORF5 are translated from distinct overlapping ORFs from the same 0.9 kb subgenomic RNA (Russo *et al.,* 1994). The protein p21 is required for viral cell-to-cell movement and p20 has been shown to be involved in symptom induction as well as being a suppressor of gene silencing (Rochon, 1991; Rochon and Xiang, personal communication). The non-coding regions at the 5' and 3' ends and those between ORFs 2 and 3 and 3 and 4 contain promoter elements involved in RNA replication and sgRNA synthesis as well as in translation of their respective downstream ORFs. It is generally accepted that CNV p33 (and its homologues in other tombusviruses) is involved in viral RNA replication. This is based on the following observations: 1) p92 cannot support viral replication in the absence of p33 in plant protoplasts (Oster *et al.,* 1998; Panaviene *et al.,*

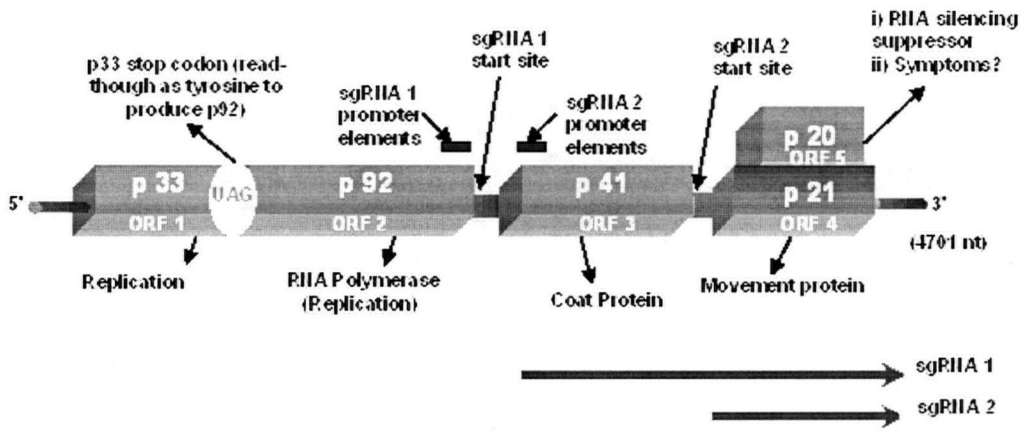

Fig.2.1. Linear representation of the CNV RNA genome structure. Boxes correspond to the five open reading frames (ORFs 1-5); the protein encoded by each ORF is indicated in yellow. p92 is expressed by translational read-through of the p33 stop codon (UAG). The initiation sites for the two subgenomic RNAs (sgRNA1 and sgRNA2) generated during CNV infection are indicated. The coat protein (p41) is expressed from sgRNA1 and p20 and p21 are expressed from different overlapping ORFs on sgRNA2. Functions for each of the proteins are indicated. The horizontal bar corresponds to the genome (4701 nt) with the 5' and 3' noncoding regions indicated.

2003); (ii) p33 binds to viral RNA *in vitro* (Panaviene *et al.*, 2003; Rajendran *et al.*, 2003) and (iii) p33 interacts with p92 *in vitro* and *in vivo* (Rajendran *et al.*, 2004).

2.2. Intracellular replication sites of plus-strand RNA viruses.

2.2.1. Association of the replicase complex with membrane-containing structures.

All characterized positive-strand RNA viruses assemble their RNA replication complexes on intracellular membranes, usually in association with membrane vesicle formation or other membrane rearrangements (Fig. 2.2,a and b) (Carette *et al.*, 2002; Lee *et al.*, 2001; Miller *et al.*, 2001; Navarro *et al.*, 2004; Restrepo-Hartwig *et al.*, 1999; Rohozinski *et al.*, 1996). The membrane associated replication complexes have been shown to contain viral RNA and both virus- and host-encoded proteins (Buck, 1996; Noueiry *et al.*, 2003). For such replication complexes, the host membrane constitutes a crucial host factor serving multiple purposes. First the membrane provides a surface on which replication factors are localized and concentrated for assembly. The membrane also surrounds and protects the viral site of replication providing an environment in which the RNA replication factors and viral RNAs are sequestered from competing host RNA templates and possibly from competing processes such as translation. This organization also helps to protect viral dsRNA replication intermediates from dsRNA-induced host defense responses such as RNA silencing or interferon-induced responses (Ahlquist *et al.*, 2003). While many positive-strand RNA viruses form similar spherical invaginations, others form distinct membrane structures, including alternate types of vesicles or appressed membranes. The detailed organization of membrane rearrangement

is not yet defined (Ahlquist *et al.*, 2003; Rust *et al.*, 2001; Schwartz *et al.*, 2002), however it has been suggested that the several apparently different membranous structures may actually represent variations of a common theme (Schwartz *et al.*, 2004).

Various (+) strand RNA viruses assemble their RNA replication complexes on different, but usually specific membranes or membrane subsets. For example, certain alphaviruses use endosomal and lysosomal membranes (Kaariainen *et al.*, 2002), the plant viruse, *Brome mosaic virus* (BMV) uses the membranes of the endoplasmic reticulum (Restrepo-Hartwig *et al.*, 1996) and *Cymbidium ringspot virus* (CyRSV) uses the membrane of the mitochondrion (Rubino *et al.*, 2001). The specific type of membrane system utilized in assembling the viral replication complex depends on the individual virus. The viral-encoded components of the replicase contain sequences that are involved in the specificity of targeting. Some viral and host components are recruited to the complex indirectly via specific interaction with a membrane targeted replicase component. (Burgyan *et al.*, 1996; Hagiwara *et al.*, 2003; Rubino *et al.*, 1998). However, the specific membrane that is targeted by the polymerase may not be critical for replication as several RNA virus replication complexes have been retargeted to other membranes without loss of function (Burgyan *et al.*, 1996; Miller *et al.*, 2003). These observations imply that host membranes are used for providing a surface on which replication factors are localized and concentrated for assembly but that specific membrane proteins themselves do not participate in the replication process.

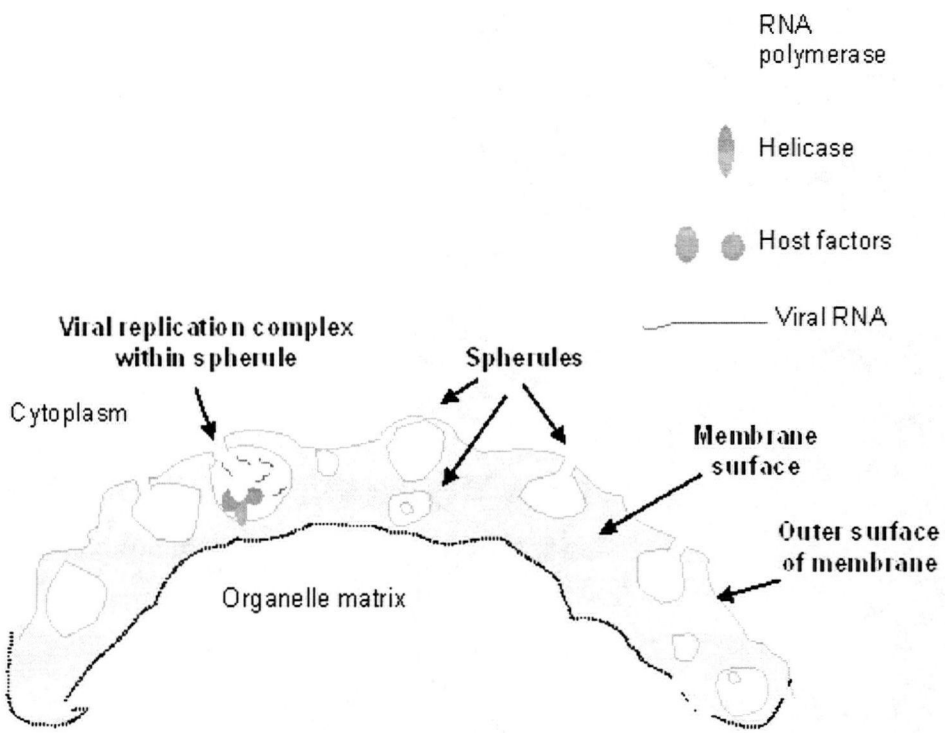

Fig. 2.2.a. Diagrammatic representation of spherules and the viral RNA replication complex. The gray area corresponds to the surface of the organelle membrane. The white invaginations at the cytoplasmic side of the membrane correspond to spherules. The closed circles also represent spherules but the plane of the section is different and therefore they appear as closed spheres (or spheres within spheres). Components of the replication complex and viral RNAs are shown along with their location within a spherule.

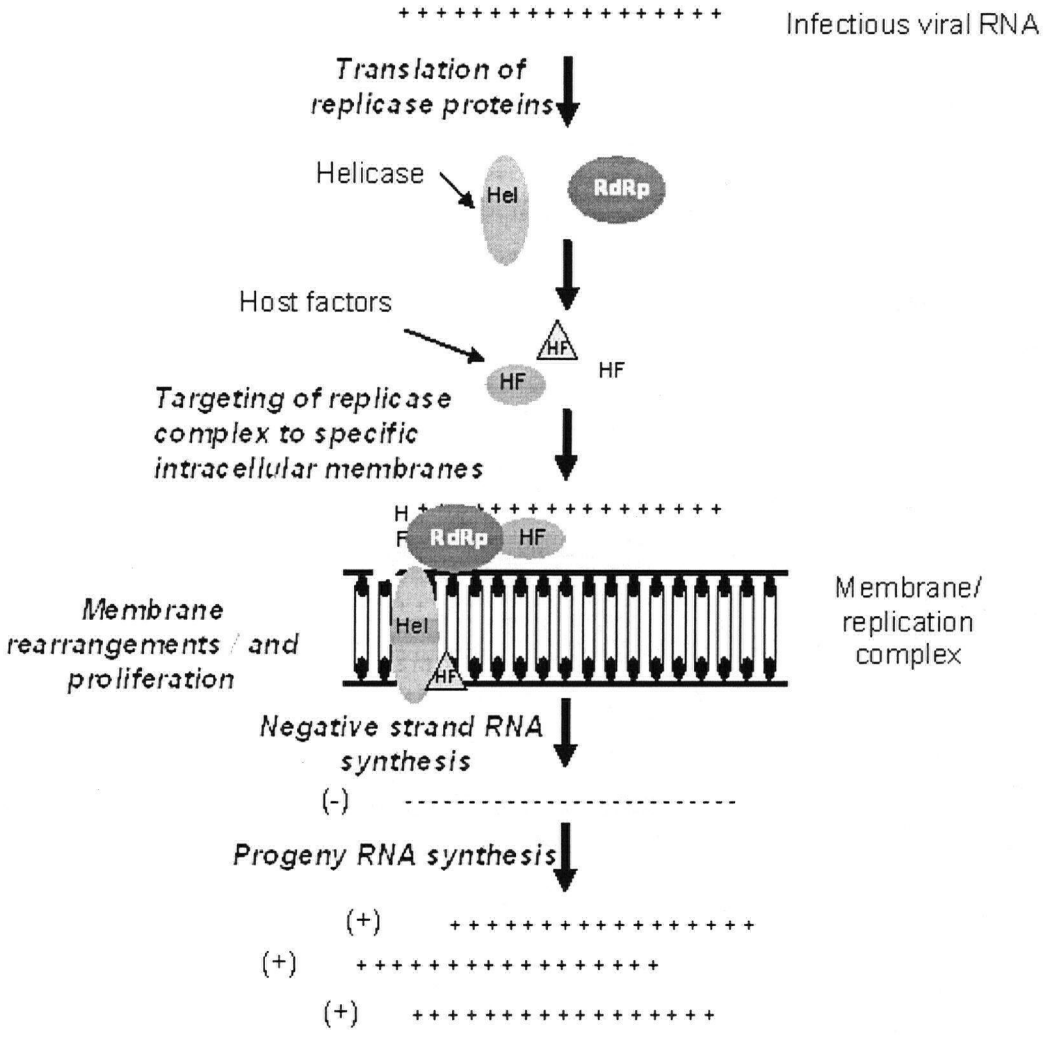

Fig. 2.2.b. A general scheme for replication of a positive-strand RNA virus. Specific steps in RNA replication are described. Following release of virion RNA translation occurs to produce proteins involved in viral genome replication. The replication complex consists of viral encoded proteins such as the RNA dependent RNA polymerase (RdRp) and helicase as well as host factors and viral RNA. The complex assembles on a specific intracellular membrane. Negative-strand RNA is synthesized from viral RNA and several plus-strand RNAs are then produced from the negative-strand template. Assembly of the replicase complex on membranes is associated with membrane proliferation and the formation of spherules (cup-shaped vesicles) within the membrane with the opening facing the cytoplasmic side.

2.2.2. Location of replication proteins in virus-infected cells.

In a number of cases (e.g., poliovirus, alphaviruses) all of the viral replication proteins are localized within the replication complex (Bienz *et al.,* 1987; Bienz *et al.,* 1992; Froshauer *et al.,* 1988; Restrepo-Hartwig *et al.,* 1996). On the other hand, for the Flavivirus Kunjin, the replicative proteins and RNA viral synthesis sites co-localize in vesicle pockets, while other nonstructural proteins are associated with modified membranes from the intermediate compartment (Mackenzie *et al.,* 1999).

In the case of *Turnip yellow mosaic* (TYMV), replication appears to occur in association with chloroplasts, where both the 66 kDa and 140 kDa replicase associated proteins are targeted (Prod'homme *et al.,* 2003). Studies showed that targeting of the 66 kDa component of the replicase to the chloroplast envelope is dependent on expression of its 140 kDa read-through protein, indicating that the read-through portion of the 140 kDa protein contains information for chloroplast targeting and that targeting of the 66 kDa protein might occur via its ability to interact with the 140 kDa protein. Targeting was found to induce clumping of chloroplasts, which is one of the typical cytological effects of TYMV infection. These results suggest that the 140 kDa protein is a key organizer of the assembly of the TYMV replication complexes and a major determinant for their chloroplastic localization and retention (Prod'homme *et al.,* 2003).

A putative N-terminal amphipathic helix (AH) in NS4B protein of hepatitis C virus (HCV) has been found to mediate membrane association and correct localization of replication complex proteins (Elazar *et al.,* 2004).

Table 2.1. Organellar origin of MVBs induced by several tombusviruses[1].

Virus	Origin of multivesicular bodies	Reference(s)
Tomato bushy stunt virus (TBSV)	Peroxisomes	(Martelli *et al.*, 1988)
Cucumber necrosis virus (CNV)	Peroxisomes	this thesis; (Rajendran *et al.*, 2004)
Eggplant mottled crinkle virus (EMCV)	Peroxisomes, vesicles in chloroplasts	(Makkouk *et al.*, 1981)
Carnation Italian ringspot virus (CIRV)	Mitochondria	(Burgyan *et al.*, 1996)
Cymbidium ringspot virus (CymRSV)	Peroxisomes and mitochondria	(Navarro *et al.*, 2004; Rubino *et al.*, 1998)

[1] This table has been partially adapted from Martelli *et al.*, 1988

2.3. Replication of tombusviruses.

2.3.1. The subcellular site of replication.

Tombusviruses are positive-strand RNA viruses of plants whose infections are typically associated with the formation of membranous cytoplasmic inclusions called multivesicular bodies (MVBs). The periphery of MVBs have been shown to contain multiple vesicles that are approximately 80-150 nm in diameter. The MVBs induced during tombusvirus infection have been shown to originate from chloroplasts, mitochondria or peroxisomes and the site of localization appears to vary with the host of the virus as well. Table 2.1 summarizes the organellar origin of tombusvirus induced MVBs and their known or presumed sites of replication. Recently, *Red clover necrotic mosaic virus* (RCNMV) replication proteins have been shown to accumulate in association with the endoplasmic reticulum (Turner *et al.*, 2004). RCNMV is not a tombusvirus but it is a member of the *Tombusviridae* family. Therefore it appears that replication on MVBs derived from chloroplasts, mitochondria or peroxisomes will not be a general feature of the site of replication of the *Tombusviridae.*

The tombusvirus *Carnation Italian ringspot virus* (CIRV) induces MVBs derived from mitochondria whereas *Cymbidium ringspot virus* (CymRSV) induces MVBs from peroxisomes (Burgyan *et al.*, 1996; Rubino *et al.*, 2001). Replacement of 600 nucleotides from the 5' region of the CIRV genome with the corresponding region of the genome of CymRSV changes the localization of MVBs from mitochondria to peroxisomes (Burgyan *et al.*, 1996) indicating that the region of the genome that specifies the site of replication is located within the 600 nt region. The 3' terminal part of the exchanged region contains

the coding information for the amino-terminal regions of the pre-read-through domains of the replicases of CIRV (p36) and CymRSV (p33). This data therefore suggested that that these portions of p36 and p33 may contain the information that determines the site of MVB formation and/or replication in CIRV and CymRSV. Later, biochemical analysis suggested that p33 is anchored to the peroxisomal membrane through a segment of ca. 7 kDa, located in the amino terminal portion of the replicase. This segment contains two hydrophobic transmembrane domains and a hydrophilic interconnecting loop (Navarro *et al.,* 2004).

2.3.2. Tombusvirus replication complexes.

Tombusviruses encode two proteins (p33 and p92) that are required for replication (Panaviene *et al.,* 2003). As described in Section 2.1, p92 is an amber read-through protein of p33. The p92 read-through region contains the conserved motifs that are characteristic of RdRps. A conserved helicase motif, typically associated with viral RNA replicases, has not been found in p92 or p33 or any of the other 3 proteins encoded by the tombusvirus genome.

The involvement of p33 in tombusvirus RNA replication (Panavas *et al.,* 2005; Panaviene *et al.,* 2003) is supported by the observation that p92 cannot support viral replication in the absence of p33 in plant protoplasts (Oster *et al.,* 1998; Panaviene *et al.,* 2003); Also, it has been shown that CNV p33 can bind to viral RNA *in vitro* which is consistent with its proposed role in viral RNA replication (Panaviene *et al.,* 2003; Rajendran *et al.,* 2003). Recently, CNV p33 has been found to form dimers or multimers via interaction with other p33 molecules or with the p33 region of p92 (Rajendran *et al.,*

2004). The RNA-binding region in p33 has been mapped to an arginine-proline-rich motif (RPR motif). Mutations within the RPR motif in p33 affected gRNA and sgRNA synthesis (Panaviene *et al.*, 2003) as well as viral RNA recombination (Panaviene *et al.*, 2003) suggesting that p33 is involved in the replication process at multiple steps. *In vitro* studies with CNV replicase preparations demonstrated that the CNV RdRp could recognize the essential viral RNA promoter sequences (Panavas *et al.*, 2002), replication enhancers, (Panavas *et al.*, 2003) and a replication silencer element (Pogany *et al.*, 2003) during RNA synthesis.

2.4. Symptom induction by plant viruses.

Virus-infected host cells undergo many defense responses that can lead to the development of disease. As viruses invade susceptible plants, they create conditions that favor systemic infections by suppressing multiple layers of innate host defenses. When viruses meddle in these defense mechanisms, which are interlinked with basic cellular functions, phenotypic changes can result that contribute to disease symptoms (Whitham *et al.*, 2004). However, although much insight into the molecular basis of virus and host interactions that lead to disease has been obtained, many aspects of the disease induction process are not understood and therefore require further study. Many virus encoded proteins or viral genome sequences confer some level of either resistance to the host defense response and/or ameliorate host disease symptoms. Such viral sequences include the coat protein, subunits of the viral replicase, non-coding regions of the genome, virus associated defective interfering RNAs, satellite viruses and certain viral-encoded suppressors of gene silencing (Simon *et al.*, 2004). With regards to host defense systems,

there are probably many different mechanisms involved, but in general terms there is a tendency towards increased local necrosis at the sites of virus infection. The hypersensitive response (HR) of plants resistant to microbial pathogens involves a complex form of programmed cell death (PCD) that differs from developmental PCD in its consistent association with the induction of local and systemic defense responses. Hypersensitive cell death is commonly controlled by direct or indirect interactions between pathogen avirulence gene products and those of plant resistance genes and it can be the result of multiple signalling pathways. Ion fluxes and the generation of reactive oxygen species commonly precede cell death, but a direct involvement of the latter seems to vary with the plant-pathogen combination (Heath, 2000). In certain strains of *Tobacco mosaic virus* (TMV) it has been shown that the host hypersensitive response is linked to the viral-encoded RdRp but in other cases TMV may induce the hypersensitive response via another gene such as the coat protein (Whitham *et al.,* 1996). Moreover, in some viruses, necrosis develops, but there is little or no restriction in virus movement as a result of the necrotic reaction and systemic necrosis develops, indicating that a different mechanism may induce the necrosis and/or the virus counter-defense strategy is more effective than the host defense strategy (Matthews, 1992). Diverse number of mechanisms may be involved in host resistance to viruses as well as in the viral anti-defense process. These processes are not only of fundamental interest to the scientific community, but their understanding could lead to new strategies for managing virus-induced disease.

3. Materials and Methods

All DNA manipulations were performed using standard techniques (Sambrook *et al.,* 1989). The sequences of polymerase chain reaction (PCR) generated DNA fragments within plasmid constructs were confirmed by sequencing and the overall structure of the final construct was confirmed by restriction enzyme analysis.

3.1. PCR amplication of p33, p20, GFP and YFP-SKL sequences.

PCR was used to amplify the p33, p20 and GFP ORFs from plasmid constructs already available in the laboratory. In the case of YFP-SKL, a commercially available construct was used (see below). The overall strategy for PCR amplification for subsequent cloning purposes was as follows: Each pair of primers (Table 3.1) corresponded to the 5' [forward primer (F)] or 3' [reverse primer; (R)] end of the respective protein coding region and also carried a restriction enzyme sequence (Table 3.1) added to the primer 5' terminus that was used for subsequent cloning of the PCR fragment (see Section 3.2). Following amplification, the PCR product was digested with the indicated restriction enzyme electrophoresed through a 1% agarose gel. The excised PCR fragment was purified using a Qiagen's QIAquick PCR purification kit. PCR was carried out as described by Fisher *et al.,* (1997).The thermal cycling parameters were; 1 cycle of 95°C for 1 minute followed by 25 cycles of 95°C for 30 seconds, 55°C for 30 seconds, 72°C for 2 minutes.

The p33 ORF was amplified using primers *Nco1*-33K-F and *Pst1*-33K-R and then digested with *Nco1* and *Pst1* and the GFP ORF was amplified using primers *Pst1*-GFP-F

and *BamH1*-GFP-R and then digested with *Pst1* and *BamH1*. The CNV p33 ORF was amplified from pK2/M5 (Rochon *et al.,* 1991) and a previous pK2/M5 construct containing GFP was used for amplification of GFP. A similar strategy was used to construct PBI525/p20/GFP except that the p20 ORF was amplified using primers *Nco1*-20K-F and *Pst1*-20K-R using pK2/M5 as template.

3.2. Plasmid construction

The *Agrobacterium tumefaciens* binary vector pBINPLUS (Van Engelen *et al.,* 1995) was the plasmid used for expression of p33- and p20-GFP fusion proteins following agroinfiltration of plant leaves. Constructs (Fig. 3.1) were prepared in two overall steps as follows. In the first step, fusion protein ORFs were cloned into the plant expression vector pBI525 (Pang *et al.,* 1992) between the dual 35-S promoter and the Nos terminator. In the second step the region between the dual 35-S promoter and the Nos terminator was transferred to pBINPLUS. The construct pBI525/p33/GFP was made by trimolecular ligation of *Nco1*- and *BamH1*-digested pBI525, and the CNV p33 and GFP PCR fragments described above. pBI525/p33/GFP was then digested with *Sal1* and *EcoR1*, which flanks the insert region, and ligated into to similarly digested pBINPLUS. A similar trimolecular ligation approach was used for construction of pBI525/p20/GFP. The *Sst1* and *Sal1* digested fragment of pBI525/p20/GFP was cloned in *Sst1* and *Sal1* digested pBINPLUS to make p20/GFP. The construct pBin/GFP was a gift from Yu Xiang, Plasmid pEYFP-peroxi with SKL peroxisomal signal peptide was purchased from Clontech (Palo Alto, CA). This was used to make the peroxisomal-marker plasmid pYFP/SKL in two steps. pEYFP-peroxi was digested with *Nco1* and *Xba1* and ligated to

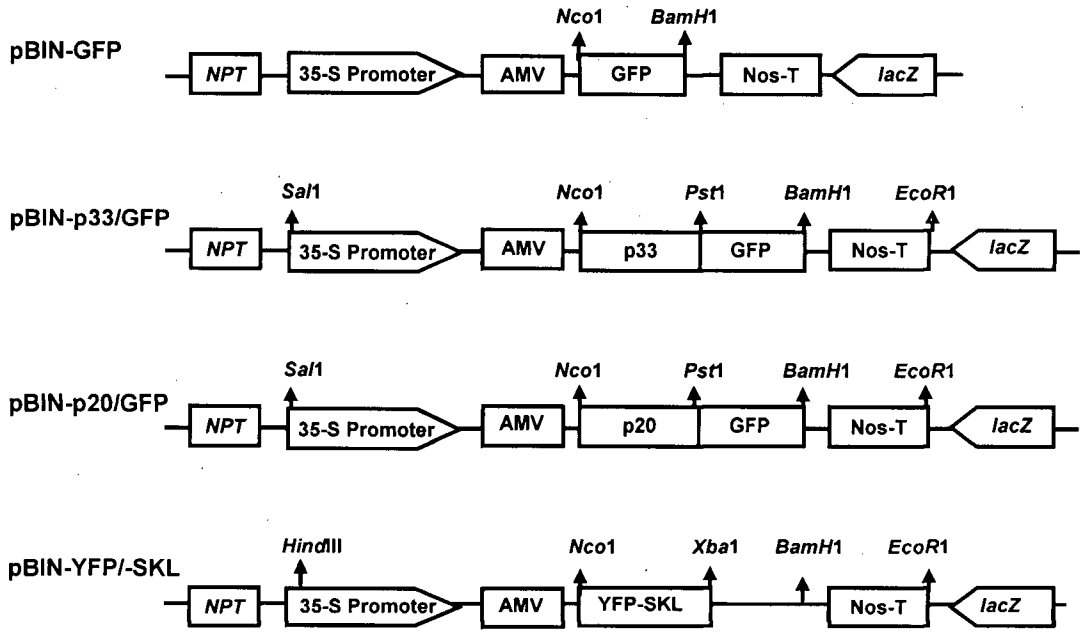

Fig. 3.1. Schematic representation of the pBINPLUS fusion protein expression constructs. CNV p33 or p20 were fused in-frame with GFP and placed downstream of the dual 35S promoter. AMV corresponds to the alfalfa mosaic virus translational enhancer and Nos to the nopaline synthase transcription termination site, *Lac Z* encodes for β-galactosidase. and NPT II is the kanamycin resistance gene used for selection of pBINPLUS in *A. tumefaciens* cultures. Individual protein sequences were amplified by PCR using the primers shown in Table 3.1 and then ligated into the intermediate vector pBI-525. In the case of the p33 and p20 GFP fusions, the ligation reaction contained pBI-525, GFP and either p33 or p20. The sequences between the dual 35S promoter to the Nos terminator were excised from pBI-525 using *SalI* and *EcoRI* and cloned into the corresponding site of pBINPLUS resulting in the construct shown above. Restriction enzyme(s) site(s) utilized in making constructs have been shown. The YFP-SKL peroxisomal marker was constructed by transfer of the gene from plasmid pEYFP-peroxi ,(Clontech) to pBI525 using restriction enzymes and cloned in pBINPLUS .

Table 3.1. Oligonucleotides used in this study (see Materials and Methods).

Primer Name	Primer Sequence	Purpose
*Nco1*_p33_F	5' CAAGACCATGGTGTGGCCTAAGAAAG3'	*Nco1* site at 5' end of p33 ORF
*Pst1*_p33 _R	5' AAGCCCTGCAGTTTCACACCAAGGGAC3'	*Pst1* site at 3' end of p33 ORF
*Pst1*_GFP_F	5' ATATACTGCAGGTGAGCAAGGGCG3'	*Pst1* site at 5' end of GFP
*BamH1*_GFP_R	5' TATTAGGATCCTTACTTGTACAGCTCGTA3'	*BamH1* site at 3' end of GFP
*Nco1*_p20_F	5' ATAAACCATGGAACGAGCTATACA3'	*Nco1* site at 5' end of P20
*Pst1*_p20_R	5' AGTCTCTGCAGCTCGCTTTCTTTA3'	*Pst1* site at 3' end of P20

similarly digested pBI525 to create pBI525/YFP/SKL. The *HindIII- EcoR1* fragment of pBI525/SKL/YFP was cloned in the corresponding site of pBINPLUS to create pYFP/SKL.

3.3. Agrobacterium-mediated transient expression

All pBINPLUS constructs were used to transform *A. tumefaciens* strain GV3101 (Koncz *et al.,* 1986) by the freeze and thaw method (Chen *et al.,* 1994). The agroinfiltration procedure was performed as described by Guo *et al.,* (2002). Transformants were streaked on LB/agar plates containing 50 µg/ml kanamycin and 10 µg/ml rifampicin and incubated at 28 °C overnight. A single colony from the plate was inoculated into 3 ml LB medium containing antibiotics as above, and grown at 28 °C for 48 h with vigorous shaking. One µl of the culture was transferred to 50 ml LB medium containing the above antibiotics, 10 mM MES, pH 5.6 and 20 µM acetosyringone. After incubation at 28 °C for 20 h with vigorous shaking, whereupon the OD_{600} of the culture had reached 1.0, the bacteria were centrifuged at 4000 g for 6 min at 4^0 C. The pellet was resuspended in 50 ml 10 mM MES, pH 5.6 and 10 mM $MgCl_2$, and then 200 µM acetosyringone was added. The bacterial suspension was incubated at room temperature for 5 h without shaking. The cultures were used to infiltrate *N. benthamiana* leaves. To maintain a uniform concentration of *Agrobacterium*, the OD_{600} of the mixtures was adjusted to 1.0–1.2. Simultaneous agroinfiltration of two different constructs was done using mixtures of individually transformed bacterial suspensions. The suspensions were mixed in a 1:1 ratio. Twenty four to thirty five hours post-infiltration, plant leaves were

examined by confocal microscopy and/or were used for protein analysis. All experiments were repeated two to four times, and the results of a representative experiment are shown.

3.4. Isolation and biochemical treatment of membranes

Cellular fractionation and biochemical treatment of membranes was done as described by Schaad *et al.*, (1997). Leaf tissues obtained from pBin/GFP or p33/GFP infiltrated *N. benthamiana* plants were used for fractionation experiments as follows. One g of leaf tissue was ground in 4 ml of buffer PEB (50 mM Tris–HCl, pH 7.4, 15 mM $MgCl_2$, 10 mM KCl, 20% glycerol, 0.1% β-mercaptoethanol, 10 mM phenyl-methyl-sulfonyl fluoride [PMSF]), and the extract was centrifuged at 3000 g at 4^0C for 10 min to pellet nuclei, chloroplasts and cell wall debris (P1). The supernatant (S1) was subjected to centrifugation at 30 000 g at 4°C for 30 min, resulting in soluble (S30) and crude membrane (P30) fractions. Analysis of protein/membrane interactions in the P30 membrane fraction was conducted using a previously described method (Schaad *et al.*, 1997) as follows. For alkaline extraction, the P30 pellet was resuspended in 0.1 M Na_2CO_3, pH 10.5, 4 mM EDTA and 4 mM PMSF. For urea extraction, the P30 pellet was resuspended in 25 mM HEPES, pH 6.8, 4 mM EDTA, 4 mM PMSF and 4 M urea. For salt extraction, the P30 pellet was resuspended in PEB buffer containing 1 M KCl. In each extraction, the samples were incubated on ice for 30 min, then subjected to centrifugation at 30 000 g at 4°C for 30 min. S30 fractions were pelleted and the pellets of P30 as well as S30 fractions were resuspended in Laemmli buffer in volumes equal. Equivalent amounts of samples were electrophoresed through an SDS-PAGE gel and analyzed by immunoblotting using anti-GFP antibodies (Clontech).

3.5. Western blot analysis

Aliquots of protein samples were electrophoresed in SDS-12% PAGE gels, and electrotransferred to a polyvinylidene difluoride membrane (PVDF, Bio-Rad). Membranes were blocked with 5% nonfat dry milk solution in Tris-buffered saline (TBS) (25 mM Tris-HCl, pH 8.0, 125 mM NaCl,) containing 0.1% Tween 20. Blocked membranes were then probed with monoclonal anti-GFP antibodies (Clontech) diluted 1:500 in TBS buffer and incubated for 1 h at room temperature This was followed by three 10-min washes with TBS and incubation for an additional 1 h at room temperature with alkaline phosphatase-conjugated goat anti-mouse antibody (Sigma) at a dilution of 1:800. Reactive protein bands were visualized with the enhanced chemiluminescence system (ECL; Amersham) according to the manufacturer's instructions.

3.6. Detection of hydrogen peroxide

Detection of hydrogen peroxide in agroinfiltrated leaves using phenol red was done as described by (Svalheim *et al.*,1993). In this assay, an increase in absorbance at 590-610 nm resulting from the peroxidase-catalyzed oxidation of phenol red by H_2O_2 is measured. Leaf discs (8 mm in diameter) from mock, pBin/GFP, pBIN/p33, pBIN/p20 agroinfiltrated or CNV infected *N. benthamiana* were washed in distilled water, blotted dry with KimWipes, floated on 1ml phenol red solution (PRS) (10 mM MES-KOH, pH 6.5, 0.56 mM phenol red, sodium salt) and incubated for 4 h in the dark in the presence of horseradish peroxidase (HRPO, type II, salt free powder, Sigma) at 8.5 U/ml. The reaction was stopped by increasing the pH to 12.5 via the addition of 10 □l of 1 N NaOH. Production of H_2O_2 by the leaf discs was assayed by measuring the OD_{590} of the phenol

red solution. Assays were conducted at 1, 2, 3, 4 and 5 days post-infiltration for each construct using 6 samples from two different leaves of the agroinfiltrated plant. The OD_{590} obtained using mock infiltrated plants was subtracted from all other values. The statistical significance of differences between values obtained for each construct in comparison to six leaves of pBin/GFP at each day was assessed using a T-test.

For histochemical determination of hydrogen peroxide levels, leaves from agroinfiltrated plants were immersed in freshly prepared 3,3'-diaminobenzidine (DAB)/HCl stain (1mg/ml, pH 3.8) in distilled water for 4 h (Thordal-Christensen *et al.*, 1997). Tissue was then cleared by immersing the leaf in boiling ethanol for 10 minutes. Leaves were then examined at 40X magnification. In the presence of hydrogen peroxide and peroxidase, DAB instantly polymerizes to a brown precipitate.

3.7. Confocal microscopy

Confocal microscopy was carried out using a Leica TCS SP2 microscope. A krypton-argon laser (488, 568 and 647-nm lines) was used to discriminate between EGFP and EYFP fluorescence. The bandwidth mirror settings for discriminating between the two signals were 493/518 (EGFP) and 585/612 (EYFP). EFYP (512 nm) and EGFP (488 nm) excitation was observed and was confirmed empirically as well. The two channels were allocated false green (EGFP) and red (EYFP) colors. GFP fluorescence was observed with standard settings (excitation wavelength 488 nm). To observe GFP fluorescence in living leaf epidermal cells, 2 cm by 2 cm samples of leaf tissue were cut from agroinfiltrated *N. benthamiana* leaves, 1 day post-infiltration. The leaf samples were

placed on a glass slide, a drop of water was applied on top of the samples and a cover slip was added.

3.8. Plant inoculations with viral RNA transcripts

Synthetic CNV genomic RNA was produced by T7 RNA polymerase run-off transcription of a *SmaI*-linearized full-length CNV infectious clone (pK2/M5) as previously described (Rochon *et al.*, 1991). Transcripts were used to inoculate four leaves of carborundum-dusted *N. benthamiana* plants at the six- to eight leaf stage. Transcripts were used to inoculate to four plants and leaves were used for peroxidase and DAB assays at 4dpi. Each experiment was repeated at least three times.

4. Results

4.1. GFP-tagged CNV p33 associates with peroxisomes in agroinfiltrated leaves of *N. benthamiana.*

The MVBs associated with tombusvirus infection have been suggested to be sites of virus replication (Appiano *et al.,* 1986; Bleve-Zacheo *et al.,* 1997; Rubino *et al.,* 2001). Electron microscopy of CNV-infected *N. clevelandii* leaves has indicated that CNV induces the formation of MVBs from peroxisomes (personal communication, D. Rochon). To assess whether CNV p33 associates with peroxisomes, the CNV p33 ORF was fused in-frame with that of GFP and placed under control of a dual 35S promoter in a binary vector (Fig. 3.1). This construct (p33/GFP) and a control construct containing the GFP ORF but lacking the p33 ORF were introduced into *N. benthamiana* leaf cells using agroinfiltration. Localization of GFP was assessed using confocal microscopy. Examination of p33/GFP agroinfiltrated cells indicated that fluorescence was associated with several small, circular, green fluorescent structures. Higher magnification clearly revealed that the subcellular structures were fluorescent at their periphery (Fig. 4.1A, panel a). The organelles were 1.2-1.5 □m in diameter, and were occasionally observed to be somewhat motile (not shown). Large aggregates of the small round structures were often observed (Fig. 4.1B, panel a). In addition, fluorescence appeared to be largely confined to the small circular structures. As expected, control cells expressing unfused GFP showed green fluorescence throughout the cytoplasm and nucleus; GFP was not seen in association with the small structures observed using p33/GFP constructs (not shown).

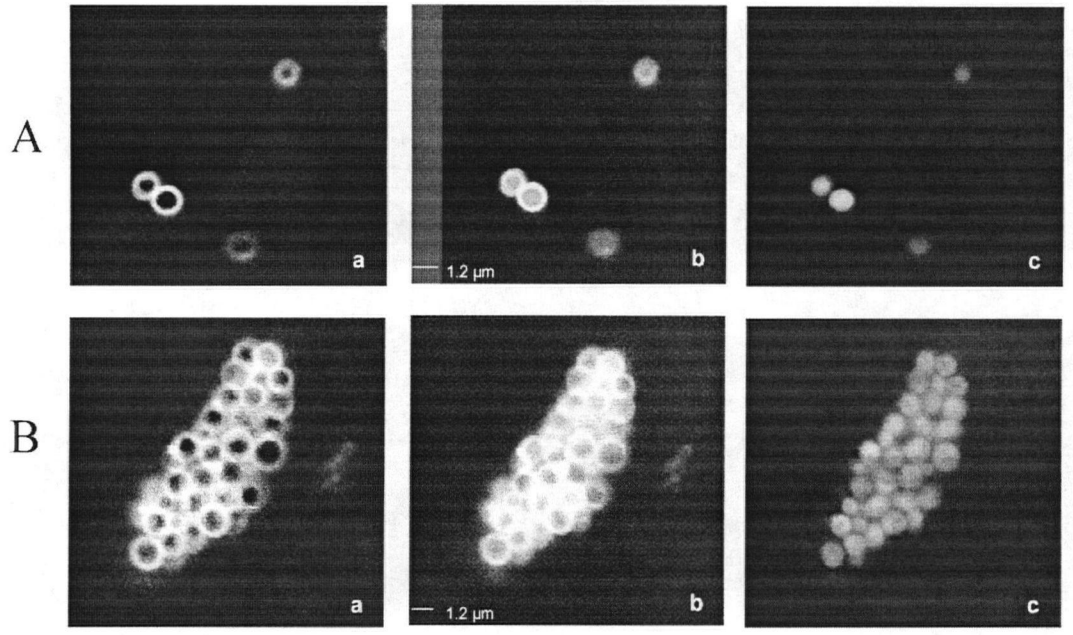

Fig. 4.1. GFP-tagged CNV p33 localizes to the peroxisomal membrane in agroinfiltrated leaves of *N. benthamiana.* The upper and lower panels show two different areas of co-infiltrated leaves. In each panel 'a' shows GFP fluorescence, 'c' shows YFP fluorescence (artificially coloured red – see Materials and Methods) and 'b' shows a merged image of both GFP and YFP fluorescence. Panel B shows an aggregate of peroxisome which was 10 □m in length.

The size and shape of the fluorescent structures detected using p33/GFP agroinfiltration are consistent with the possibility that they represent peroxisomes. The scanning micrographs using merged images of the green fluorescence and the red autofluoroscence of chloroplasts showed that these spherical structures were present in the vicinity of chloroplasts (not shown).To assess if the structures do represent peroxisomes, *N. benthamiana* leaves were co-infiltrated with p33/GFP and pYFP/SKL. The latter construct expresses yellow fluorescent protein (YFP) and targets to peroxisomes due to the presence of a C-terminal serine-lysine-leucine (SKL) tripeptide which is known to target proteins to the peroxisomal matrix (Titorenko *et al.,* 2001). Since some overlap exists between the fluorescence spectra of GFP and YFP, it was necessary to exclude fluorescence emissions where the overlap occurs. Also, since the yellow and green fluorescence is difficult to differentiate by eye, yellow fluorescence was artificially coloured red. Leaves co-infiltrated with p33/GFP and pYFP/SKL showed co-localization of green and yellow fluorescence to the small circular organelles (Fig. 4.1A and B, panels b and c) observed in p33/GFP infiltrations (Fig. 4.1A and B, panels a) indicating that p33/GFP targets to peroxisomes. Notably, however, fluorescence produced by p33/GFP was found only in association with the periphery of peroxisomes and not with the peroxisomal matrix as was observed in pYFP/SKL infiltrations (see Fig. 4.1A and B, panels a and c). Aggregates of peroxisomes were often observed in p33/GFP infiltrated leaves (Fig. 4.1B, panels a-c). The same level of aggregation in pYFP/SKL infiltrated leaves was not observed (not shown) raising the speculation that the aggregation may be specifically due to p33/GFP expression in the peroxisome membrane.

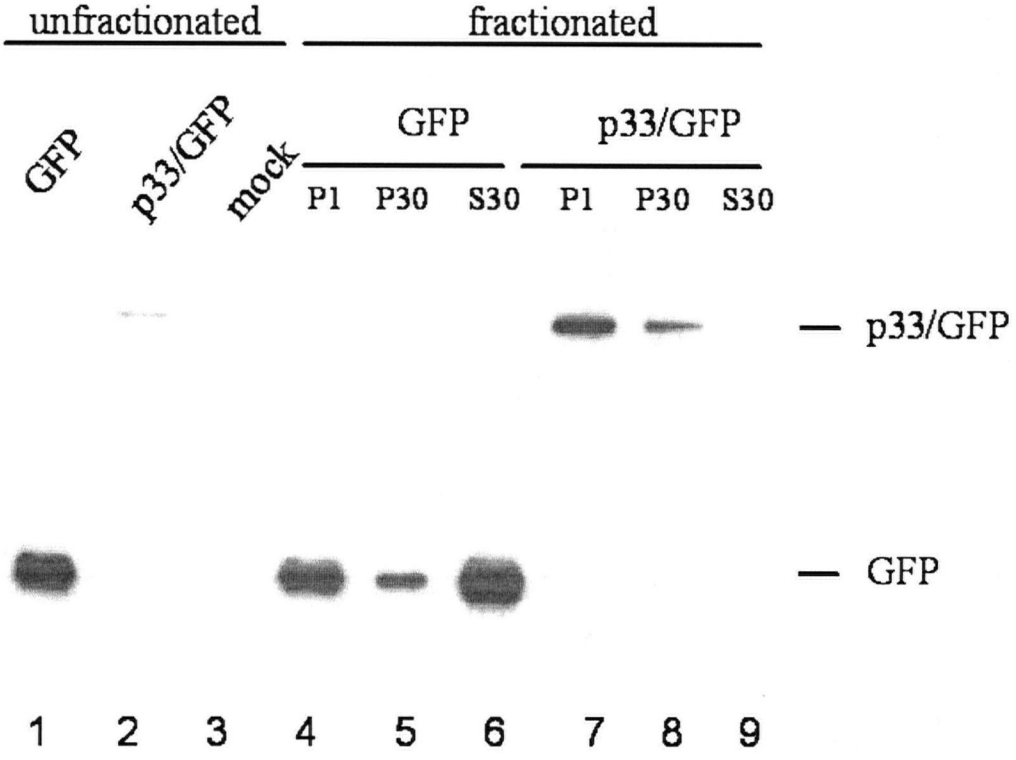

Fig. 4.2. The p33/GFP fusion protein associates with membranes in infiltrated *N. benthamiana* plants. Extracts of leaf tissue infiltrated with GFP or p33/GFP were electrophoresed through a 12% SDS-PAGE gel and then blotted and probed with a GFP monoclonal antibody. Lanes 1-3 show total leaf extracts of GFP-, p33/GFP- and mock-infiltrated leaves. Lanes 4-6, show the P1, P30 and S30 fractions of GFP-infiltrated leaves and lanes 7-9 those of p33/GFP-infiltrated leaves. The P1 and P30 lanes contain 5% of the total leaf extract whereas the S30 lane represents 3.75 % of the total leaf extract. The position of GFP and the p33/GFP fusion protein is indicated on the right. Molecular mass standards (BenchMark™ , Invitrogen) (not shown) were used to confirm that the bands correspond to the predicted GFP or p33/GFP fusion protein mass.

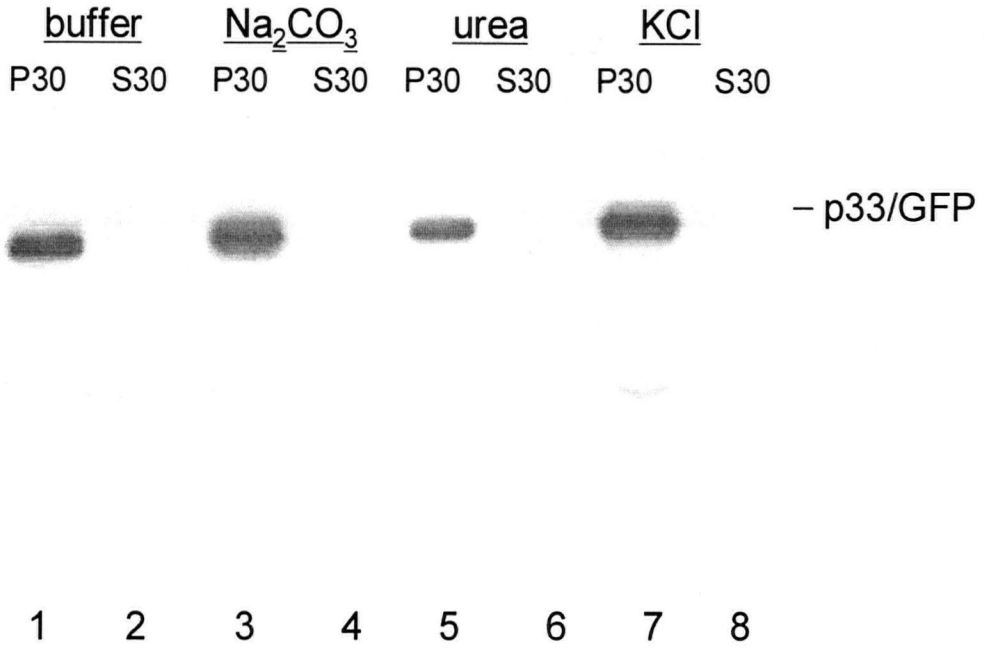

Fig. 4.3. The p33/GFP fusion protein is tightly associated with membranes. The P30 fraction of CNV p33/GFP infiltrated leaves was either not treated (lanes 1 and 2) or treated with 0.1 M Na_2CO_3 (lanes 3 and 4), 4 M urea (lanes 5 and 6) or 1 M KCl (lanes 7 and 8). Following treatment, extracts were centrifuged at 30,000 g and aliquots of the pellet (P30) and supernatant (S30) were electrophoresed, blotted onto PVDF membranes and detected with a GFP monoclonal antibody. Approximately equal amounts of each sample were analyzed. The position of the p33/GFP fusion protein is indicated on the right. Molecular mass standards (BenchMark™ , Invitrogen) (not shown) were used to confirm that the band corresponded to the predicted p33/GFP fusion protein.

Our results thus far suggest that p33 may be specifically associated with the peripheral membranes of peroxisomes in CNV infections.

4.2. The p33/GFP fusion protein associates with membranes in infiltrated plants.

The confocal microscopy results suggest that CNV p33 associates with peroxisomal membranes. To further ascertain the membrane localization of p33, cellular fractionation experiments were conducted using leaf tissue obtained from agroinfiltrated *N. benthamiana* plants. Leaves from plants infiltrated with p33/GFP were homogenized, filtered and separated into P1, P30 and S30 fractions using centrifugation. The P1 fraction is enriched for nuclei and may also contain some intact cellular organelles. The P30 fraction consists primarily of smaller organelles and endoplasmic reticulum and the S30 fraction predominantly soluble cellular material. Aliquots of each fraction were then electrophoresed though a SDS-PAGE gel and the association of p33/GFP with different fractions was assessed by Western blot analysis using a GFP monoclonal antibody for detection. Fig. 4.2 shows that the p33/GFP fusion protein is predominantly in the P30 fraction (compare lanes 7-9). Unfused GFP was found primarily in the S30 fraction as expected (Fig. 4.2, compare lanes 4-6). The association of p33/GFP with the P30 fraction is consistent with the results obtained using confocal microscopy where p33/GFP was found to be on the periphery (membranes) of peroxisomes. It is noted that the p33/GFP protein was also found in the P1 fraction. This may be due to the presence of large aggregates of peroxisomes that were often observed in p33/GFP infiltrated plants (Fig. 4.1, panel B). p33/GFP was not found to be associated with the S30 fraction. This is

unexpected as some organellar breakage is expected to occur during leaf extraction and the S30 fraction would be expected to contain the membranes of the broken organelles. .

4.3. The p33/GFP fusion protein is tightly associated with membranes

To further analyze the association of p33/GFP with membranes, the P30 fraction was treated with either 1 M KCl, 4 M urea or 0.1 M Na_2CO_3, pH 10.5. These treatments are expected to dislodge proteins that are weakly or peripherally associated with membranes. Following treatment, the extracts were centrifuged at 30,000 g and protein associated with the P30 pellet (membrane) and P30 supernatant (soluble) fractions were assessed using SDS-PAGE analysis followed by Western blotting using a GFP monoclonal antibody for detection. It can be seen in Fig. 4.3 that p33/GFP was found only in the pellet fraction of each of the treatments. These results show that p33/GFP is tightly associated with cellular membranes. Taken together, our results support the notion that CNV p33 associates with the peroxisomal membrane as an integral protein in infected plants.

4.4. *N. benthamiana* leaves agroinfiltrated with p33/GFP develop necrotic-like patches.

During the course of the experiments involving agroinfiltrations, we noted that the surface of p33/GFP infiltrated leaves frequently contained necrotic-like patches. Since CNV infected *N. benthamiana* typically produces necrotic symptoms, we further examined the p33/GFP infiltrated leaves for the possible presence of necrosis as this observation suggested to us that p33 may contribute to the induction of necrosis during

CNV infections. To do this, several *N. benthamiana* plants were agroinfiltrated with p33/GFP. Fig. 4.4 (panel d) shows a typical result, wherein a p33/GFP infiltrated leaf contains necrotic-like patches. Experiments using mock- and pBin/GFP-infiltrated leaves did not produce the necrotic-like patches. The necrotic-like symptoms typically became visible 4-5 days post-infiltration and were only observed in the cells of *N benthamiana* agroinfiltrated leaves that were confirmed by fluorescence microscopy to be expressing p33/GFP (not shown). Leaves infiltrated with pYFP/SKL were also examined and necrosis was not observed (data not shown), and therefore it is unlikely that the p33/GFP induced necrotic-like reaction is due to a non-specific effect of overexpression of p33/GFP in peroxisomes of agroinfiltrated *N. benthamiana.*

4.5. Phenol red assays to assess hydrogen peroxide production in leaf samples do not show a clear correlation between necrosis and levels of peroxide accumulation in control and p33/GFP infiltrated plants.

Many previous studies have implicated increased peroxide accumulation in the development of necrosis in pathogen infected plants (Levine *et al.,* 1994). Since peroxide metabolism occurs within peroxisomes (Titorenko *et al.*, 2001), we wished to assess whether the necrotic like patches in p33/GFP infiltrated plants were associated with increased levels of peroxide, possibly as a result of the association of p33/GFP with peroxisomes. An assay utilizing phenol red was used to quantify peroxide levels in p33/GFP infiltrated *N. benthamiana* leaves as previously described (Svalheim *et al.*, 1993). As shown in Fig. 4.5, p33/GFP infiltrated leaves appear to show slightly higher levels of peroxide than pBin/GFP infiltrated leaves at 3-4 days post-infiltration. A T-test

analysis was therefore conducted and the results of this analysis indicated that statistically significant differences between pBin/GFP and p33/GFP infiltrated plants occur at 3 and 4 days post-infiltration. Significant differences were also found between pBin/GFP and CNV at 4 and 5 days post-infiltration. However, the level of peroxide accumulation in p33/GFP and CNV was very small in comparison to that obtained in another study that used specific elicitors from cell walls of *Phythophthora megasperma* (Svalheim and Robertsen, 1993). Of considerable significance to the observations made here, is the finding that GFP infiltrated plants accumulate very high levels of peroxide even when p33 is absent. Therefore the observations described in Fig. 4.5 appear to be largely due to either the presence of *A. tumefaciens,* pBin itself, or the high levels of GFP protein produced during agroinfiltration. Therefore, further experiments will need to be conducted to examine the potential role of peroxide accumulation in the development of necrosis in p33/GFP infiltrated plants (see Discussion).

Fig. 4.4. *N. benthamiana* leaves agroinfiltrated with p33/GFP develop necrotic-like patches. Panels a-d show mock-, GFP-, CNV p20/GFP- and CNV p33/GFP- infiltrated leaves. Photographs were taken at 4 days post infiltration.

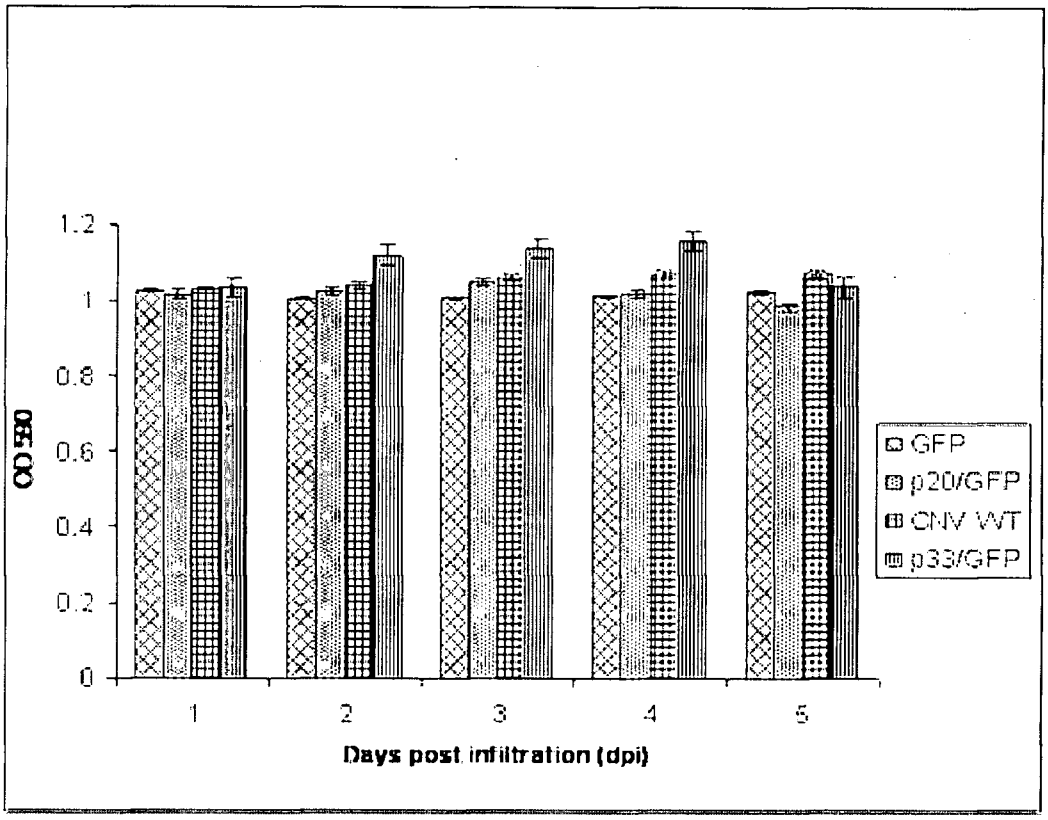

Fig. 4.5. p33/GFP infiltrated *N. benthamiana* leaves show a modest increase in the levels of hydrogen peroxide. Bars indicate the OD_{590} obtained following the phenol red bioassay for measuring H_2O_2 production in leaves. Each bar corresponds to the average of six treatments from two separate leaves in one experiment. Lines above the bar indicate the standard deviation. The numbers below each set of bars correspond to the number of days post-infiltration (or post-inoculation in the case of CNV) of the indicated construct. Values obtained from mock-inoculated leaves were subtracted from each treatment prior to statistical analysis. A t-test was conducted to determine if there are any statistically significant differences between the values obtained for the various constructs (see Results section).

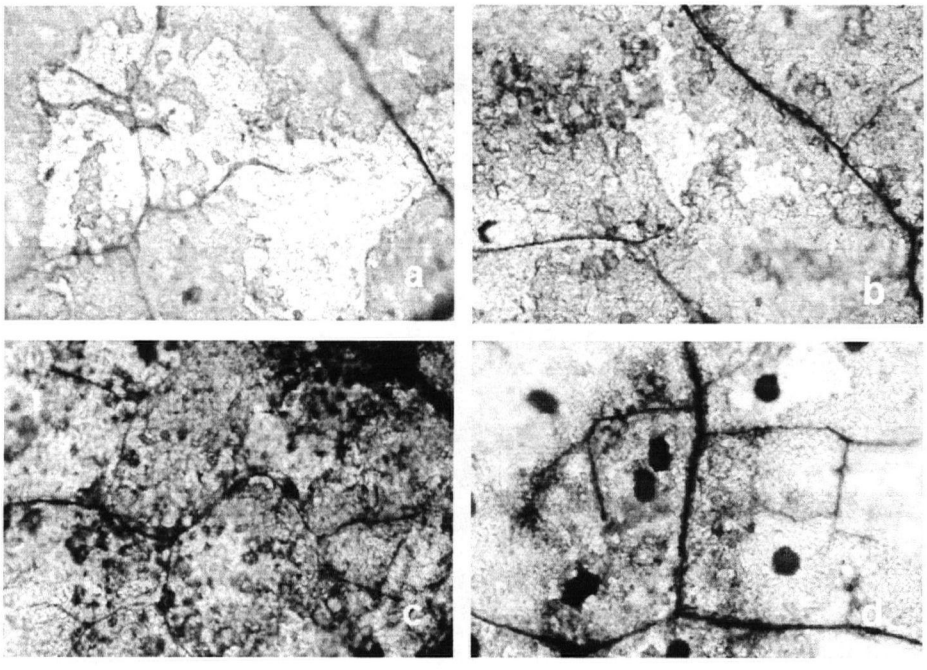

Fig. 4.6. p33/GFP infiltrated leaves accumulate peroxide as determined by DAB staining: Panel a shows GFP- and panel b shows p20/GFP-agroinfiltrated leaves. Panels c and d show CNV-inoculated and p33/GFP-agroinfiltrated leaves. Take-up and polymerization of DAB is indicated by the reddish-brown staining in the leaf tissue and signifies the production of hydrogen peroxide.

An additional experiment to assess the possibility of increased hydrogen peroxide production was done using the DAB (3,3'-diaminobenzidine) uptake method for *in vivo* detection of H_2O_2 production in leaves (Thordal-Christensen *et al.*, 1997). This procedure that has been widely used for assessing the involvement of increased peroxide production in the necrotic reaction of pathogen infected plants. In this procedure, peroxide production is measured by the take-up and polymerization of DAB in necrotic tissue which can be observed by examining leaves for the presence of dark-red staining. It can be seen in Fig. 4.6 (panels c and d) that staining does occur in the vascular tissue of both p33/GFP infiltrated leaves and in CNV-infected leaves (Fig. 4.6). The possibility that this observation relates to disruption of peroxisome function in p33/GFP agroinfiltrated or CNV infected plants will be discussed.

4.6. *N. benthamiana* leaves agroinfiltrated with p20/GFP do not develop necrotic-like patches.

Previous experiments have suggested that the CNV p20 protein is involved in the production of necrosis in infected plants (Rochon *et al.*, 1991). Similar experiments conducted with the homologous protein (p19) of the related virus, *Tomato bushy stunt virus* (TBSV) have also indicated that this protein is responsible for inducing necrosis (Scholthof *et al.*, 1995a). However, in both cases, the effect of p20/p19 was determined by expression of the protein from a viral genome and therefore the interpretation of the effect could be influenced by other viral factors. Since our results with p33/GFP infiltrations indicated that p33/GFP may be responsible for inducing necrosis in plants, we wished to further evaluate the role of CNV p20 in inducing necrosis by expressing

p20 via agroinfiltration and independent of viral infection or expression of other viral-encoded proteins. The subcellular location of CNV p20 was first assessed by agroinfiltration of a p20 GFP fusion protein (p20/GFP) in *N. benthamiana* leaves. Confocal microscopy of agroinfiltrated leaves indicated that the fusion protein was diffusely distributed in the cytoplasm with no apparent association with cellular organelles (data not shown). CNV p20/GFP infiltrated leaves were also examined as with p33/GFP infiltrated tissue for: 1) the production of necrosis on inoculated leaves; 2) increased production of H_2O_2 using the Phenol Red method and 3) increased H_2O_2 production using DAB staining. It can be seen in Fig. 4.4, (panel b) that p20/GFP infiltrated plants do not develop obvious signs of necrosis. In addition, in Fig. 4.5 and Fig. 4.6, (panel b) no evidence for increased H_2O_2 production was obtained (this was confirmed using a t-test analysis). These results indicate that under these experimental conditions and with the criteria used for assessing necrosis, that necrosis is not directly induced by p20 expression.

5. Discussion

Viral genome replication plays a pivotal role in the life cycle of the virus and constitutes a critical step in viral disease development. The aim of the present study was to determine the subcellular location of the replicase associated CNV p33 in cells of *N. benthamiana* as part of a longer term goal to identify the cellular site of CNV replication. While previous biochemical studies have shown that CNV p33 (and its homologs in other tombusviruses) is associated with viral replication complexes (Nagy *et al.,* 2000; Panaviene *et al.,* 2004; Scholthof *et al.,* 1995) the intracellular location of CNV p33 with cellular membranes during the course of CNV replication had not yet been determined at the onset of this study.

5.1 CNV p33/GFP targets to peroxisomes in agroinfiltrated plants.

It has previously been shown that the N-terminal half of ORF1 (p33) of two tombusviruses, CIRV(p36) and CyRSV (p33), contain the determinants for the formation of MVBs (Burgyan *et al.,* 1996; Rubino *et al.,* 1998). The replicase proteins of these viruses have been shown to have MVBs derived from mitochondria and peroxisomes. (Burgyan *et al.,* 1996). The thought that the peripheral vesicles of MVBs are the site of tombusvirus replication was derived from the observation that they: 1) appear in infected cells before virus particle accumulation (Appiano *et al.,* 1981), contain fibrillar material consisting of double stranded RNA (Di Franco *et al.,* 1984; Russo *et al.,* 1983); 3) incorporate [^{3}H] uridine (Appiano *et al.,* 1986) and 4) contain viral replicase proteins (Bleve-Zacheo *et al.,* 1997). Electron microscopy (EM) of CNV-infected tissues show

MVBs originating from a subcellular organelle which appeared to be a peroxisome since some of the MVBs contained what appeared to be crystals of catalase (personal communication, D. Rochon). The data described in this thesis demonstrates that the replicase-associated CNV p33 indeed targets to peroxisomes. Additionally, it is shown here, via confocal analysis, that targeting to the membrane of peroxisomes occurs. Taken together, our confocal and EM studies suggest that the membrane of peroxisomes is a possible site for assembly of the CNV replicase complex and that this assembly leads to the formation of MVBs. However, the manner in which p33 induces proliferation of membrane is not known.

5.2 CNV p33 is an integral membrane protein

Verification and characterization of the membrane association of CNV p33 was conducted by cellular fractionation experiments (Fig. 4.2) where it was found that p33/GFP was specifically associated with the membrane fraction, but not the supernatant fraction. Further treatment of the P30 membrane fraction under conditions known to remove weakly bound proteins showed that p33/GFP was resistant to this treatment indicating that p33 has an integral membrane protein. Recently, CymRSV p36 (Navarro *et al.,* 2004) and CNV p33 (Panavas *et al.,* 2005) were shown to be targeted to peroxisomes when expressed in yeast cells. However, the experiments described here were conducted in plant cells and therefore provide more convincing information regarding the actual site of p33 targeting in a plant host. The data provided here can also be interpreted to indicate that the cellular mechanisms underlying peroxisome targeting sites in cells is conserved among yeast and plants.

5.3 CNV p33 does not contain a clearly identifiable peroxisome targeting signal.

The peroxisomal targeting signals differ according to whether the peroxisomal proteins are destined to the matrix or to the membrane (Rachubinski *et al.*, 1995). Most peroxisomal matrix proteins contain a PTS1 signal consisting of the C-terminal tripeptide SKL (or essentially constitutes a tripeptide from the consensus sequence (S/T/A/G/C/N)-(K/R/H)-(L/I/V/M/A/F/Y), whereas only a few have the N-terminal PTS2 signal which consists of the nonapeptide (R/K)(L/V/I)$(X)_5$(H/Q)(L/A). Examination of the CNV p33 sequence indicates that it contains neither a PTS1 nor a PTS2 signal. The membrane PTS (mPTS) involved in targeting peroxisomal membrane proteins is not defined, since a consensus sequence has not yet been identified. However, one to several transmembrane domains and stretches of positive amino acids in the proximity of the domains have been shown to be required. Many integral membrane proteins are synthesized on free polysomes in the cytosol and post-translationally targeted to, and inserted into, the peroxisomal membrane. This process involves (in order): (1) protection of hydrophobic transmembrane segments of membrane proteins from aggregation and maintenance of their import-competent conformations during and after synthesis in the cytosol; (2) targeting of proteins to the peroxisomal membrane which is mediated by targeting signals of the mPTS1 type and/or cytosolic receptor(s); (3) docking to the peroxisomal membrane, which involves membrane-bound proteins and (4) ATP hydrolysis-independent insertion of proteins into the peroxisomal membrane, followed by their assembly within the membrane (see review by Titorenko *et al.*, 2001 and references therein).

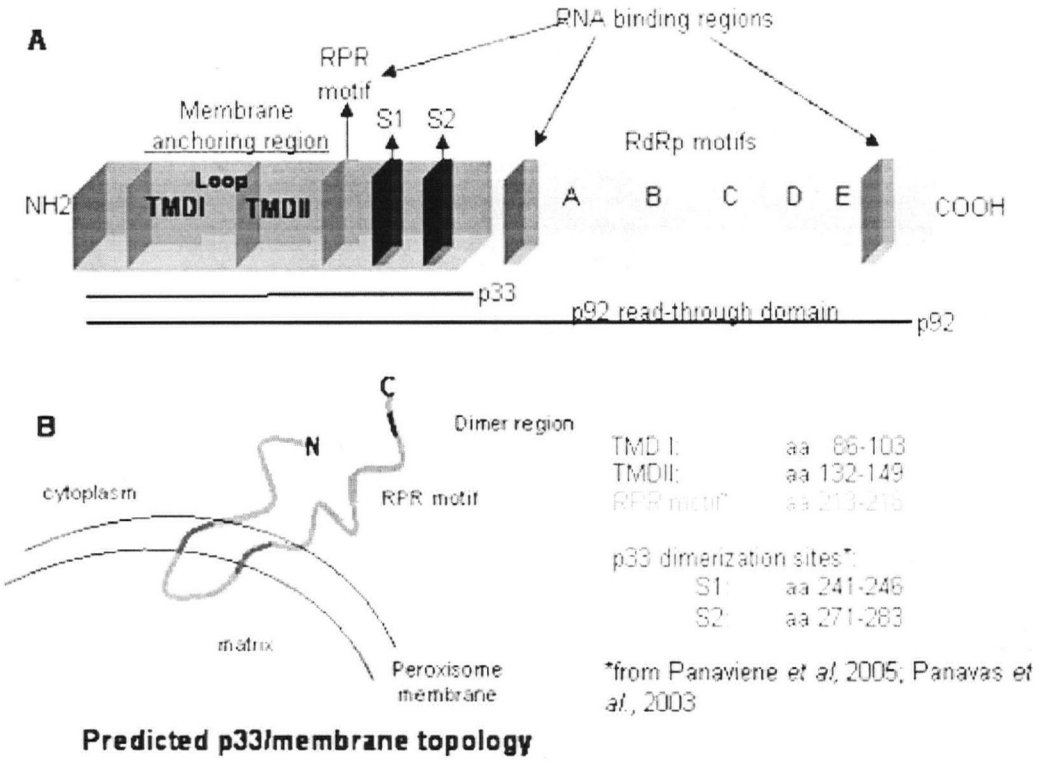

Fig. 5.1.CNV p33 has two predicted transmembrane domains. Putative transmembrane domains (TMD) were predicted using the program HMMTOP (Tusnády *et al.,* 2001; http://www.enzim.hu/hmmtop). (A) Diagrammatic representation of p92 indicating the location of TMDI and TMDII, a 29 aa hydrophilic "loop" between the domains, the RNA binding domains (includes the RPR motif) and the p33:p33 and p33:p92 dimerization regions. The numbers in the blue box indicate the position of the TMDs in the p33 protein RNA binding domain and p33:p33/p92 interaction domains are as predicted by Panavas *et al.,* 2005. (B)Topology of CNV p33 in the peroxisome membrane based on HMMTOP predictions is shown. The HMMTOP "out" prediction is interpreted to mean the cytoplasmic face of the organelle and the "in" prediction the inside or matrix of the organelle. The colouring scheme for the various domains is as in (A).

Computer analysis of the 295 aa p33 sequence using the HMMTOP program described by Tusnady *et al.,* (2001) suggested the presence of two 17 aa hydrophobic domains long enough to span the membrane of peroxisomes. The N- and C-terminal regions were predicted to be on the "outside" of the membrane and therefore are interpreted as being on the cytoplasmic side of the membrane. This orientation is consistent with our suggestion that CNV p33 could be a transmembrane protein (Fig.5.1). A further prediction from the computer analysis is that the two TMDs are separated by a 29 aa hydrophilic loop which may protrude into the peroxisomal matrix (i.e., predicted by HMMTOP to be "inside"). It has recently been shown that CNV p33 contains 3 RNA binding motifs and also two regions involved in p33:p33 and p33:p92 dimerization (Panavas *et al.,* 2005). A diagram summarizing the location of the various predicted domains on the linear sequence of p33 is shown in Fig. 5.1. In addition a schematic illustration of the potential topology of p33 with respect to the peroxisomal membrane is also shown.

Several analyses have failed to indicate that CNV p33/GFP contains any conspicuous peroxisomal targeting region despite the fact that p33/GFP is clearly associated with peroxisomes in agroinfiltrated plants. This is similar to the findings reported by (Navarro *et al.,* 2004)) regarding CymRSV p33 localization signals wherein obvious consensus signals thought to be characteristic of proteins targeted to peroxisomes were not evident. Panavas *et al.,* (2005) found that the p33 N-terminal sequence does not affect its subcellular localization to peroxisomes in yeast, however it was found to play an important role in tombusvirus replication

While membrane association is possibly a universal feature of positive-strand viral RNA replication, the mechanisms involved in targeting replication proteins and templates to specific intracellular membranes are largely unknown (Salonen *et al.*, 2005). Determining the peroxisome membrane targeting signal in CNV p33 is an important area of research as it will provide further insight into membrane targeting signals as well as furthering the understanding of the structure and function of CNV p33.

5.4 CNV p33 may be involved in the induction of necrosis in infected plants.

CNV infected *N. benthamiana* plants typically develop necrotic lesions on inoculated leaves and systemic symptoms develop at about 4-5 days post-inoculation. Necrosis, blackening and curling occurs at the base of the new leaves that were just developing at the time of inoculation. Symptoms then spread to other parts of the plant and to other leaves and eventually the plant succumbs to systemic necrosis. During our experiments directed towards localization of CNV p33 in cells, we noted that agroinfiltration of CNV p33/GFP in *N. benthamiana* leaves is associated with the formation of necrotic-like symptoms in leaves (Fig. 4.4). Using genetically engineered CymRSV and CIRV hybrid viruses indirect evidence has been obtained that the products of ORF1 in these viruses (equivalent to CNV p33) may play a significant role in the induction of necrosis while hybrids containing chimeric ORF1 were not able to induce lethal necrosis. It was also shown that elicitation of the necrotic phenotype requires the presence of both p33 and p19 (the equivalent of CNV p20) (Burgyan *et al.*, 2000). In addition, studies with *Cucumber leafspot virus* (CLSV), an aureusvirus that is closely related to the tombusviruses, showed that infections where p27 and p82 (the homologs of

CNV p33 and p92) are the only CLSV proteins expressed, exhibit severe necrosis (Reade *et al.,* 2002). Thus our data in conjunction with reports by of Burgyan *et al.,* (2000) and Reade *et al.,* (2002) suggest that p33 may be a determinant for necrosis among tombusviruses and aureusviruses.

Previous work with CNV suggested that p20 is responsible for the development of necrosis. This was based on the observation that whereas infections with WT CNV in plants was associated with severe necrosis, plants infected with CNV p20 knock-out mutants failed to develop necrotic symptoms (Rochon *et al.,* 1991). Similar results were obtained with other tombusviruses (Russo *et al.,* 1994) as well as with the closely related aureusviruses (Reade *et al.,* 2002). However, these experiments did not directly test p20 for its ability to induce necrosis, as p20 expression was always within the context of virus infection. The results of the p20/GFP agroinfiltration experiments (Fig. 4.4) show that p20 expression in leaves (in the absence of virus infection) does not result in observable necrotic symptoms. Therefore it seems likely that p20, on its own, does not induce symptoms during virus infection and, moreover, that p33 may instead be involved.

The tombusvirus p20 protein has been demonstrated to be a powerful suppressor of the antiviral gene silencing response in plants through its ability to bind siRNAs (Voinnet, 2005). This property is regularly exploited by researchers to increase expression of foreign genes in plants via agroinfiltration (Voinnet, 2005), and to our knowledge there have been no reports that its use in agroinfiltration induces necrosis. This reinforces our observation that CNV p20 does not induce necrosis and indirectly supports the notion that p33 may be involved instead. We do not know why knock-out mutants of p20 in tombusviruses result in attenuation of necrosis. However, given that

p20 is a suppressor of the gene silencing pathway, we propose that infections that lack p20 allow the host defense system to silence CNV viral RNA (through degradation) and thereby reduce levels of p33 expression and resultant necrosis.

In TMV, the helicase domain of replicase protein has been shown to induce the N-mediated defense response in tobacco (Erickson *et al.*,1999). CNV p33 is important for CNV replication but it does not contain the motifs that are characteristic of viral helicases. Our results suggest that CNV p33 induces necrosis but that the presence of a helicase domain is not required.

5.5 Does CNV p33 expression in *N. benthamiana* result in hydrogen peroxide production?

Using hydrogen peroxide assays we have shown that CNV p33/GFP agroinfiltrated tissues accumulate statistically higher levels of hydrogen peroxide (H_2O_2) compared to GFP or p20/GFP inoculated plants. In addition, necrotic tissue from CNV-infected plants also accumulates higher levels of H_2O_2. However, in both cases, the increased level of peroxide production was very low in comparison to published studies using a similar method (Svalheim and Robertson, 1993), so the biological significance of the increased peroxide levels will require additional studies.

Many different viral proteins have been identified as inducing symptoms in plants. These include the helicase domain of TMV (Erickson *et al.*, 1999), the p19 protein of TBSV (Scholthof *et al.*,1995) and the TMV coat protein (Culver, 2002). There are probably many different mechanisms involved in the host response and the virus/host interaction leading to symptom development. Hydrogen peroxide (H_2O_2) is an often-

used biological indicator for programmed cell death (Mittler *et al.*, 1998). H_2O_2 from the oxidative burst plays a key role in the orchestration of a localized hypersensitive response during the expression of plant disease resistance (Levine *et al.*, 1994). The peroxisomes contain enzymes that use molecular oxygen to oxidize various substrates, forming hydrogen peroxide (H_2O_2). Catalase, also a peroxisome-localized enzyme, efficiently decomposes H_2O_2 into H_2O (Lopez-Huertas *et al.*, 2000). H_2O_2 has been suggested to be a signaling molecule for the induction of the hypersensitive reaction (Dat *et al.*, 2003; Kwon *et al.*, 2003; Vandenabeele *et al.*, 2003). Intracellular concentrations of H_2O_2 can be quantified spectrophotometrically by oxidation of the dye, phenol red (Svalheim *et* and Robertson, 1993) or by histochemical staining by DAB (Thordal-Christensen *et al.*, 1997. These assays have been used to measure levels of H_2O_2 in necrotic tissue resulting from pathogen infection. In experiments to assess accumulation of H_2O_2, spectrophotometric quantification using the phenol red assay indicated that H_2O_2 levels were statistically significantly higher in p33/GFP infiltrated leaves compared to pBin/GFP at 3 (p= 0.0159) and 4 (p=0.0002) days post-infiltration. However, no statistically significant differences were found between pBin/GFP and p20/GFP infiltrated leaves at any day. Statistically significant differences in the levels of peroxide were also observed in comparisons between pBin/GFP infiltrated and CNV-infected tissue at the 4th (p= 0.00221 and 5th (p = 0.0482) day of the assay. Our data also suggest that H_2O_2 levels progressively increased in p33/GFP infiltrated tissues from 3 to 4 days, and a statistical analysis confirmed that the difference was significant. However, there was a considerable production of hydrogen peroxide in leaves when pBin/GFP itself was inoculated (see Fig. 4.5). Phenol red assays to assess hydrogen peroxide production in

leaf samples failed to show a convincing correlation between necrosis and high levels of peroxide accumulation in control and p33/GFP infiltrated plants or CNV infected plants.. However, DAB staining with p33/GFP and CNV inoculated leaves at 4 dpi indicated peroxide accumulation occurred in p33/GFP infiltrated and CNV infected plants but not control plants (Fig 4.6). The association of CNV p33 with peroxisomes and its ability to induce necrosis-like symptoms in infiltrated plants suggests that p33 may contribute to the necrotic-like reaction via disruption of peroxisomal function, but the involvement of peroxide accumulation in the induced necrosis will require further experimentation.

DAB staining was visible prior to detectable necrosis (Fig. 4.6). This suggests that increased levels of peroxide are associated with the subsequent necrosis. A time course of the DAB staining would be a useful means for further examining the correlation between hydrogen peroxide levels and necrosis. Using the phenol red assay an overall increase in the average level of peroxide was apparent from 1-4 dpi but then at 5 dpi levels appeared to drop. The drop at 5 dpi in hydrogen peroxide levels could be due to death of the cell tissues. These results indicate that expression of CNV p33/GFP in *N. benthamiana* leaves brought about an increase of hydrogen peroxide that preceded cell death. However it should be noted that using the phenol red assay the amount hydrogen peroxide accumulation was much lower than that observed in other similar studies using elicitors or pathogens (Svalheim and Robertson, 1993; Malolepsza *et al.*, 2005). Therefore further experimentation to explain the basis for the necrosis produced in p33/GFP inoculated plants is required.

Our results (Fig. 4.1) show that p33/GFP agroinfiltration is associated with aggregation of peroxisomes. The aggregation of the peroxisomes could result from

extensive dimerization (Fig 5.1) (Panavas *et al.,* 2005) of membrane bound p33 from different peroxisomes. Regardless of the basis for peroxisomal aggregation, it is not known if aggregation occurs in natural CNV infections or if aggregation is merely a reflection of overexpression of p33 in cells.

Recently it has been shown that the CNV coat protein (CP) targets to chloroplasts in *N. benthamiana* cells and that this targeting may reflect the site of CNV particle disassembly (Rochon, unpublished observations). It is interesting to note that the R domain of the CNV coat protein, which binds virion RNA, has a putative peroxisomal targeting sequence. It is possible that after virus disassembly the coat protein may assist in viral RNA targeting to peroxisomes for subsequent replication.

Recently, it has been predicted that threshold levels of CNV p33 are required for recruitment of the viral RNA into replication complexes (Pogany *et al.,* 2005). Also, in CIRV, the level of viral RNA replication was shown to be proportional to RNA polymerase levels and depended on a threshold concentration of p36 (Pantaleo *et al.,* 2004). CNV p33 is one of the first proteins synthesized in virus infected cells and it is usually present at 20 times the level of its read-through product, p92 (Scholthof *et al.,* 1995). When p33 is expressed in the cell it causes severe necrosis of the plant tissues as shown in our experiments. High amounts of CNV p33 may therefore destroy cells even before the virus is able to complete its life cycle. Therefore, when expressed in the context of virus infection, it is likely that the amount of p33 synthesized is regulated by the other viral genes to ensure that virus can complete its replicative cycle.

Taken together, the data described in this thesis suggest that replicase-associated CNV p33 localizes to peroxisomes. In addition, the data suggest that p33 appears to be

responsible, on its own, for the induction of necrosis in CNV infected cells. It is possible that increased levels of peroxide in p33 agroinfiltrated leaves as determined by DAB staining suggests that the necrosis may be a result of increased peroxide production. Further experiments will be required to strengthen and validate these suggestions.

Bibliography

1. Ahlquist, P., Noueiry, A., Lee, W. M., Kushner, D. B. & Dye, B. T. (2003). Host factors in positive-strand RNA virus genome replication. *J Virology* 77, 8181-8186.

2. Appiano, A., D'Agostino, G., Bassi, M., Barbieri, N., Viale, G. & Dell'Orto, P. (1986). Origin and function of tomato bushy stunt virus-induced inclusion bodies. II. Quantitative electron microscope autoradiography and immunogold cytochemistry. *J Ultrastructure Res* 97, 31-38.

3. Appiano, G., D'Agostino, P., A, R. & Pennazio, S. (1981). Sequence of cytological events during the process of local lesion formation in the tomato bushy stunt virus-Gomphrena globosa hypersensitive system. *J Ultrastructure Res* 76, 173-180.

4. Bienz, K., Egger, D. & Pasamontes, L. (1987). Association of polioviral proteins of the P2 genomic region with the viral replication complex and virus induced membrane synthesis as visualized by electron microscopic immunocytochemistry and autoradiography. *Virology* 160.

5. Bienz, K., Egger, D., Pfister, T. & Troxler, M. (1992). Structural and functional characterization of the poliovirus replication complex. *J Virol* 66, 2740-2747.

6. Bleve-Zacheo, T., Rubino, L., Melillo, M. T. & Russo, M. (1997). The 33K protein encoded by cymbidium ringspot tombusvirus localizes to modified peroxisomes of infected cells and of uninfected transgenic plants. *J Plant Path* 79, 197-202.

7. Buck, K. W. (1996). Comparison of the replication of positive-stranded RNA viruses of plants and animals. *Adv Virus Res* 47, 159–251.

8. Burgyan, J., Rubino, L. & Russo, M. (1996). The 5'-terminal region of a tombusvirus genome determines the origin of multivesicular bodies. *J Gen Virol* 77, 1967-1974.

9. Burgyan, J., Hornyik, C., Szittya, G., Silhavy, D. & Bisztray, G. (2000). The ORF1 products of tombusviruses play a crucial role in lethal necrosis of virus-infected plants. *J Virology* 74, 10873-10881.

10. Carette, J. E., Van Lent, J., MacFarlane, S. A., Wellink, J. & Van Kammen, A. (2002). Cowpea mosaic virus 32- and 60-kilodalton replication proteins target and change the morphology of endoplasmic reticulum membranes. *J Virol* 76, 6293-6301.

11. Chen, H., Nelson, R. S. & Sherwood, J. L. (1994). Enhanced recovery of transformants of *Agrobacterium tumefaciens* after freeze-thaw transformation and drug selection. *Biotechniques* 16, 664-668, 670.

12. Culver, J. N. (2002). Tobacco mosaic virus assembly and disassembly: determinants in pathogenicity and resistance. *Annu Rev Phytopathol* 40, 287-308.

13. Dat, J. F., Pellinen, R., Beeckman, T., Kangasjärvi, J., Langebartels, C., Inzé, D. & Van Breusegem, F. (2003). Changes in hydrogen peroxide homeostasis trigger an active cell death process in tobacco. *Plant J* 33, 621-632.

14. Di Franco, A., Russo, M. & Martelli, G. P. (1984). Ultrastructure and origin of MVBsinduced by carnation Italian ringspot virus. *J Gen Virol* 65, 1233-1237.

15. Elazar, M., Liu, P., Rice, C. M. & Glenn, J. S. (2004). An N-terminal amphipathic helix in hepatitis C virus (HCV) NS4B mediates membrane association, correct localization of replication complex proteins, and HCV RNA replication. *J Virol* 78, 11393-11400.

16. Erickson, F., Holzberg, S., Calderon-Urrea, A., Handley, V., Axtell, M., Corr C. & Baker, B. (1999). The helicase domain of the TMV replicase proteins induces the N-mediated defence response in tobacco. *Plant J* Apr;18(1), 67-75.

17. Fisher, L. C. & Pei, G. K. (1997). Modification of PCR based Site –Directed Mutagenesis Method. *Biotechniques* 23, 570-574.

18. Froshauer, S., Kartenbeck, J. & Helenius, A. (1988). Alphavirus RNA replicase is located on the cytoplasmic surface of endosomes and lysosomes. *J Cell Biol* 6, 2075-2086.

19. Guo, H. S. & Ding, S. W. (2002). A viral protein inhibits the long range signaling activity of the gene silencing signal. *The EMBO Journal* 21, 398-407.

20. Hagiwara, Y., Komoda, K., Yamanaka, T., Tamai, A., Meshi, T., Funada, R., Tsuchiya, T., Naito, S. & Ishikawa, M. (2003). Subcellular localization of host and viral proteins associated with tobamovirus RNA replication. *The EMBO J* 22, 344-353.

21. Heath, M. C. (2000). Hypersensitive response-related death. *Plant Mol Biol* Oct;44(3), 321-334.

22. Kaariainen, L. & Ahola, T. (2002). Functions of alphavirus nonstructural proteins in RNA replication. *Prog Nucleic Acid Res Mol Biol* 71, 187-222.

23. Koncz, C. & Schell, J. (1986). The promoter of Ti-DNA gene controls the tissue-specific expression of chimaeric genes by a novel type of *Agrobacterium* binary vector. *Mol Gen Genet* 204, 383-396.

24. Kwon, S. H., Pimentel, D. R., Remondino, A., Sawyer, D. B. & Colucci, W. S. (2003). H_2O_2 regulates cardiac myocyte phenotype via concentration-dependent activation of distinct kinase pathways. *J Mol Cell Cardiol* 35, 615-621.

25. Lee, S. K., Dabney-Smith, C., Hacker, D. L. & Bruce, B. D. (2001). Membrane activity of the southern cowpea mosaic virus coat protein: the role of basic amino acids, helix-forming potential, and lipid composition. *Virology* 291, 299-231.

26. Levine, A., Tenhaken, R., Dixon, R. & Lamb, C. (1994). H2O2 from the oxidative burst orchestrates the plant hypersensitive disease resistance response. *Cell* 79, 583-593.

27. Lopez-Huertas, E., Charlton, W. L., Johnson, B., Graham, I. A. & Baker, A. (2000). Stress induces peroxisome biogenesis genes. *The EMBO Journal* 19, 6770-6777.

28. Mackenzie, J. M., Jones, M. K. & Westaway, E. G. (1999). Markers for trans-Golgi membranes and the intermediate compartment localize to induced membranes with distinct replication functions in flavivirus-infected cells. *J Virol* 73.

29. Makkouk, K. M., Koenig, R. & Leseman, D. E. (1981). Characterization of a tombusvirus isolated from eggplant. *Phytopathology* 71, 572-577.

30. Malolepsza U, Rozalska S. Nitric oxide and hydrogen peroxide in tomato resistance. Nitric oxide modulates hydrogen peroxide level in o-hydroxyethylorutin-induced resistance to Botrytis cinerea in tomato.Plant Physiol Biochem. 2005 Jun;43(6):623-35.

31. Martelli, G. P., Gallitelli, D. & Russo, M. (1988). *Tombusviruses*. New York: Plenum Publishing Corp.

32. Matthews, REF 1992. *Fundamentals of Plant Virology.* Academic Press, NY. 403 pp.

33. Miller, D. J., Schwartz, M. D. & Ahlquist, P. (2001). Flock house virus RNA replicates on outer mitochondrial membranes in Drosophila cells. *J Virology* 75, 11664-11676.

34. Miller, D. J., Schwartz, M. D., Dye, B. T. & Ahlquist, P. (2003). Engineered retargeting of viral RNA replication complexes to an alternative intracellular membrane. *J Virol* 77, 12193-12202.

35. Mittler, R., Feng, X. & Cohen, M. (1998). Post-transcriptional suppression of cytosolic ascorbate peroxidase expression during pathogen-induced programmed cell death in tobacco. *Plant Cell* 10, 461-473.

36. Nagy, P. & Pogany, J. (2000). Partial purification and characterization of Cucumber necrosis virus and Tomato bushy stunt virus RNA-dependent RNA polymerases: similarities and differences in template usage between tombusvirus and carmovirus RNA-dependent RNA polymerases. *Virology* 276 (2), 279–288.

37. Navarro, B., Rubino, L. & Russo, M. (2004). Expression of the Cymbidium ringspot virus 33-kilodalton protein in Saccharomyces cerevisiae and molecular dissection of the peroxisomal targeting signal. *J Virology* 78, 4744-4752.

38. Noueiry, A. O. & Ahlquist, P. (2003). Brome mosaic virus RNA replication: revealing the role of the host in RNA virus replication. *Annu Rev Phytopathol* 41, 77-98.

39. Oster, S. K., Wu, B. & White, K. A. (1998). Uncoupled expression of p33 and p92 permits amplification of tomato bushy stunt virus RNAs. *J Virol* 72, 5845-5851.

40. Panavas, T., Pogany, J. & Nagy, P. D. (2002). Internal initiation by the cucumber necrosis virus RNA-dependent RNA polymerase is facilitated by promoter-like sequences. *Virology* 296, 275-287.

41. Panavas, T. & Nagy, P. D. (2003). Yeast as a model host to study replication and recombination of defective interfering RNA of Tomato bushy stunt virus. *Virology* 314(1), 315–325.

42. Panavas, T., Hawkins C.M., Panaviene Z. & Nagy P.D. (2005). The role of the p33:p33/p92 interaction domain in RNA replication and intracellular localization of p33 and p92 proteins of Cucumber necrosis tombusvirus. *Virology* 338, 81-95.

43. Panaviene, Z., Baker, J. M. & Nagy, P. D. (2003). The overlapping RNA-binding domains of p33 and p92 replicase proteins are essential for tombusvirus replication. *Virology* 308, 191-205.

44. Panaviene, Z. & Nagy, P. D. (2003). Mutations in the RNA-binding domains of tombusvirus replicase proteins affect RNA recombination *in vivo*. *Virology* 317, 359-372.

45. Panaviene, Z., Panavas, T., Serva, S. & Nagy, P. D. (2004). Purification of the cucumber necrosis virus replicase from yeast cells: role of coexpressed viral RNA in stimulation of replicase activity. *J Virol* 78, 8254-8263.

46. Pang, S. Z., Nagpala, P., Wang, M., Slightom, J. L. & Gonsalves, D. (1992). Resistance to heterologous isolates of tomato spotted wilt virus in transgenic tobacco expressing its nucleocapsid protein gene. *Phytopathology* 82, 1223-1229.

47. Pantaleo, V., Rubino, L. & Russo, M. (2004). The p36 and p95 replicase proteins of Carnation Italian ringspot virus cooperate in stabilizing defective interfering RNA. *J Gen Virol* 85, 2429-2433.

48. Pogany, J., Fabian, M. R., White, K. A. & Nagy, P. D. (2003). A replication silencer element in a plus-strand RNA virus. *The EMBO Journal* 22, 5602-5611.

49. Pogany, J., White, K. A. & Nagy, P. D. (2005). Specific binding of tombusvirus replication protein p33 to an internal replication element in the viral RNA is essential for replication. *J Virol* 79, 4859-4869.

50. Prod'homme, D., Jakubiec, A., Tournier, V., Drugeon, G. & Jupin, I. (2003). Targeting of the turnip yellow mosaic virus 66K replication protein to the chloroplast envelope is mediated by the 140K protein. *J Virol* 77, 9124-9135.

51. Rachubinski, R. A. & Subramani, S. (1995). How proteins penetrate peroxisomes. *Cell* 83, 525-528.

52. Rajendran, K. S. & Nagy, P. D. (2003). Characterization of the RNA-binding domains in the replicase proteins of tomato bushy stunt virus. *J Virology* 77, 9244-9258.

53. Rajendran, K. S. & Nagy, P. D. (2004). Interaction between the replicase proteins of Tomato bushy stunt virus *in vitro* and *in vivo*. *Virology* 326, 250-261.

54. Rajendran, K. S. & Nagy, P. D. (2005). Kinetics and functional studies on interaction between the replicase proteins of Tomato Bushy Stunt Virus: Requirement of p33:p92 interaction for replicase assembly. *Virology* Oct 19.

55. Reade, R., Miller, J., Robbins, M., Xiang, Y. & Rochon, D. (2002). Molecular analysis of the cucumber leafspot virus genome. *Virus Research* 91, 171-179.

56. Restrepo-Hartwig, M. A. & Ahlquist, P. (1996). Bromo mosaic virus helicase- and polymerase-like proteins colocalize on the endoplasmic reticulum at sites of viral RNA synthesis. *J Virology* 70, 8908-8916.

57. Restrepo-Hartwig, M. A. & Ahlquist, P. (1999). Brome mosaic virus RNA replication proteins 1a and 2a colocalize and 1a independently localizes on the yeast endoplasmic reticulum. *J Virol* 73, 10303-10309.

58. Rochon, D. M. & Tremaine, J. H. (1989). Complete nucleotide sequence of the cucumber necrosis virus genome. *Virology* 169, 251-259.

59. Rochon, D. M. & Johnston, J. C. (1991). Infectious transcripts from cloned cucumber necrosis virus cDNA: evidence for a bifunctional subgenomic mRNA. *Virology* 181, 656-665.

60. Rohozinski, J. & Hancock, J. M. (1996). Do light-induced pH changes within the chloroplast drive turnip yellow mosaic virus assembly. *J Gen Virol* 77, 163-165.

61. Rubino, L. & Russo, M. (1998). Membrane targeting sequences in tombusvirus infections. *Virology* 252, 431-437.

62. Rubino, L., Weber-Lotfi, F., Dietrich, A., Stussi-Garaud, C. & Russo, M. (2001). The open reading frame 1-encoded ('36K') protein of Carnation Italian ringspot virus localizes to mitochondria. *J Gen Virol* 82, 29-34.

63. Russo, M., Di Franco, A. & Martelli, G. P. (1983). The fine structure of cymbidium ringspot virus infections in host tissues. III. Role of peroxisomes in the genesis of multivesicular bodies. *J Ultrastructure Res* 82, 52-63.

64. Russo, M., Burgyan, J. & Martelli, G. P. (1994). Molecular biology of tombusviridae. *Adv Virus Res* 44, 381-428.

65. Rust, R. C., Landmann, L., Gosert, R., Tang, B. L., Hong, W., Hauri, H. P., Egger, D. & Bienz, K. (2001). Cellular COPII proteins are involved in production of the vesicles that form the poliovirus replication complex. *J Virol* 75, 9808-9818.

66. Salonen, A., Ahola, T. & Kaariainen, L. (2005). Viral RNA replication in association with cellular membranes. *Curr Top Microbiol Immunol* 285, 139-173.

67. Sambrook, J., Fritsch, E. F. & Maniatis, T. (1989). *Molecular cloning: a laboratory manual.* Cold Spring Harbor Laboratory, Cold Spring Harbor, N.Y.

68. Schaad, M. C., Jensen, P. E. & Carrington, J. C. (1997). Formation of plant RNA virus replication complexes on membranes: role of an endoplasmic reticulum-targeted viral protein. *The EMBO Journal* 16, 4049-4059.

69. Scholthof KB, Scholthof H.B & A.O, J. (1995). The tomato bushy stunt virus replicase proteins are coordinately expressed and membrane associated. *Virology* 208, 365-369.

70. Scholthof, H. B., Scholthof, K. B. & Jackson, A. O. (1995). Identification of tomato bushy stunt virus host-specific symptom determinants by expression of individual genes from a potato virus X vector. *Plant Cell* Aug;7(8), 1157-1172.

71. Schwartz, M., Chen, J., Janda, M., Sullivan, M., Den Boon, J. & P., A. (2002). A positive-strand RNA virus replication complex parallels form and function of retrovirus capsids. *Mol Cell* Mar;9(3), 505-514.

72. Schwartz, M., Chen, J., Lee, W. M., Janda, M. & Ahlquist, P. (2004). Alternate, virus-induced membrane rearrangements support positive-strand RNA virus genome replication. *Proc Natl Acad Sci U S A* 101, 11263-11268.

73. Simon, A. E., Roossinck, M. J. & Havelda, Z. (2004). Plant virus satellite and defective interfering RNAs: new paradigms for a new century. *Annu Rev Phytopathol* 42, 415-437.

74. Svalheim, O. & Robertsen, B. (1993). Elicitation of H2O2 production on cucumber hypocotyl segements by oligo-1,4-a-D-galacturonides and an oligo-ß-glucan preparation from cell walls of Phythophthora megasperma f.sp. glycinea. *Physiologia Plantarum* 88, 675-681.

75. Thordal-Christensen, H., Zhang, Z., Wei, Y. & Collinge, D. B. (1997). Subcellular localization of H2O2 in plants. H2O2 accumulation in papillae and hypersensitive response during the barley powdery mildew interaction. *Plant J* 11, 1187-1194.

76. Titorenko, V. I. & Rachubinski, R. A. (2001). The life cycle of the peroxisome. *Nature Reviews Molecular Cell Biology* 2, 357-368.

77. Turner, K. A., Sit, T. L., Callaway, A. S., Allen, N. S. & Lommel, S. A. (2004). Red clover necrotic mosaic virus replication proteins accumulate at the endoplasmic reticulum. *Virology* 320, 276-290.

78. Tusnády, G. E. & Simon, I. (2001). The HMMTOP transmembrane topology prediction server. *Bioinformatics* 17, 849-850.

79. Van Engelen, F. A., Molthoff, J. W., Conner, A. J., Nap, J. P., Pereira, A. & Stiekema, W. J. (1995). pBINPLUS: an improved plant transformation vector based on pBIN19. *Transgenic Res* 4, 288-290.

80. Vandenabeele, S., Van Der Kelen, K., Dat, J. & other authors (2003). A comprehensive analysis of hydrogen peroxide-induced gene expression in tobacco. *Proc Natl Acad Sci U S A* 100, 16113-16118.

81. Voinnet, O. (2005). Non-cell autonomous RNA silencing. *FEBS Lett* Oct 31, 5858-5871.

82. Whitham, S., McCormick, S. & Baker, B. (1996). The N gene of tobacco confers resistance to tobacco mosaic virus in transgenic tomato. *Proc Natl Acad Sci* Aug 6;93(16), 8776-8781.

83. Whitham, S. A. & Wang, Y. (2004). Roles for host factors in plant viral pathogenicity. *Curr Opin Plant Biol* Aug;7(4), 365-371.